JOURNAL OF GEOPHYSICAL RESEARCH, VOL. 104, NO. D5, PAGES 5765–5784, MARCH 20, 1999

Dimethyl sulfide oxidation in the equatorial Pacific: Comparison of model simulations with field observations for DMS, SO_2, H_2SO_4(g), MSA(g), MS, and NSS

D. Davis,[1] G. Chen,[1] A. Bandy,[2] D. Thornton,[2] F. Eisele,[3] L. Mauldin,[3] D. Tanner,[3] D. Lenschow,[3] H. Fuelberg,[4] B. Huebert,[5] J. Heath,[5] A. Clarke,[5] and D. Blake[6]

Abstract. Reported here are results from an airborne photochemical/sulfur field study in the equatorial Pacific. This study was part of NASA's Global Tropospheric Experiment (GTE) Pacific Exploratory Mission (PEM) Tropics A program. The focus of this paper is on data gathered during an airborne mission (P-3B flight 7) near the Pacific site of Christmas Island. Using a Lagrangian-type sampling configuration, this sortie was initiated under pre-sunrise conditions and terminated in early afternoon with both boundary layer (BL) as well as buffer layer (BuL) sampling being completed. Chemical species sampled included the gas phase sulfur species dimethyl sulfide (DMS), sulfur dioxide (SO_2), methane sulfonic acid $(MSA)_g$, and sulfuric acid $(H_2SO_4)_g$. Bulk aerosol samples were collected and analyzed for methane sulfonate (MS), non-sea-salt sulfate (NSS), Na^+, Cl^-, and NH_4^+. Critical non-sulfur parameters included real-time sampling of the hydroxyl radical (OH) and particle size/number distributions. These data showed pre-sunrise minima in the mixing ratios for OH, SO_2, and H_2SO_4 and post-sunrise maxima in the levels of DMS, OH, and H_2SO_4. Thus, unlike several previous studies involving coincidence DMS and SO_2 measurements, the Christmas Island data revealed that DMS and SO_2 were strongly anticorrelated. Our "best estimate" of the overall efficiency for the conversion of DMS to SO_2 is 72±22%. These results clearly demonstrate that DMS was the dominant source of SO_2 in the marine BL. Using as model input measured values for SO_2 and OH, the level of agreement between observed and simulated BL H_2SO_4(g) profiles was shown to be excellent. This finding, together with supporting correlation analyses, suggests that the dominant sulfur precursor for formation of H_2SO_4 is SO_2 rather than the more speculative sulfur species, SO_3. Optimization of the fit between the calculated and observed H_2SO_4 values was achieved using a H_2SO_4 first-order loss rate of 1.3×10^{-3} s^{-1}. On the basis of an estimated total "wet" aerosol surface area of 75$\mu m^2/cm^3$, a H_2SO_4 sticking coefficient of 0.6 was evaluated at a relative humidity of ≈95%, in excellent agreement with recent laboratory measurements. The Christmas Island data suggest that over half of the photochemically generated SO_2 forms NSS, but that both BL NSS and MS levels are predominantly controlled by heterogeneous processes involving aerosols. In the case of MS, the precursors species most likely responsible are the unmeasured oxidation products dimethyl sulfoxide (DMSO) and methane sulfinic acid (MSIA). Gas phase production of MSA was shown to account for only 1% of the observed MS; whereas gas phase produced H_2SO_4 accounted for ~20% of the NSS. These results are of particular significance in that BL-measured values of the ratio MS/NSS have often been used to estimate the fraction of NSS derived from biogenic DMS and to infer the temperature environment where DMS oxidation occurred. If our conclusions are correct and both products are predominantly formed from complex and still poorly characterized heterogeneous processes, it would suggest that for some environmental settings a simple interpretation of this ratio might be subject to considerable error.

[1]School of Earth and Atmospheric Sciences, Georgia Institute of Technology, Atlanta.
[2]Department of Chemistry, Drexel University, Philadelphia, Pennsylvania.
[3]National Center for Atmospheric Research, Boulder, Colorado.
[4]Meteorology Department, Florida State University, Tallahassee.
[5]Department of Oceanography, University of Hawaii, Honolulu.
[6]Chemistry Department, University of California,Irvine.

Paper number 1998JD100002.
0148-0227/99/1998JD100002$09.00

1. Introduction

Since the early 1970s when *Lovelock et al.* [1972], and subsequently *Andreae and Raemdonck* [1983]; *Andreae and Barnard* [1984]; and *Andreae et al.* [1985], identified the presence of large marine releases of dimethyl sulfide (DMS), efforts have been underway to determine the quantitative relationship between this species and atmospheric sulfate levels. Early laboratory chamber studies revealed that sulfur in the +IV state, as SO_2, was one of the more significant products formed [e.g., *Niki et al.*, 1983; *Grosjean*, 1984;

Hatakeyama et al., 1985]. In still other kinetic studies, SO_2 was shown to undergo further oxidation (both in the gas and liquid phases), forming sulfur + VI. Thus, it could be argued that an overall qualitative picture of the chemistry of DMS seems to be in hand. Even so, the quantitative mechanistic details by which SO_2 is formed under atmospheric conditions remain poorly understood, as does the variability in this efficiency with changing conditions.

In principle, such information might be expected to fall out from laboratory chamber studies involving DMS. However, as noted in a recent review of DMS chemistry by *Berresheim et al.* [1995], a major difficulty with interpreting chamber data is the fact that nearly all studies of this type are set up with abnormally high levels of key atmospheric constituents such as NO. In many cases these have been orders of magnitude higher than those actually found in the marine boundary layer (MBL), leading to significant alterations in the mechanism. Equally important have been the mechanistic complications resulting from the limited size of the chambers themselves. This has led to reaction surface-to-volume ratios that have been orders of magnitude higher than those found in the MBL. Thus, to date, chamber studies have been somewhat limited in their ability to deliver quantitative mechanistic information related to the DMS oxidation process [e.g., *Turnipseed and Ravishankara*, 1993; *Berresheim et al.*, 1995].

Prior to the very recently published ground-based Christmas Island results by *Bandy et al.* [1996], no DMS-SO_2 field data have been reported which have shown a clearly defined causal relationship between these two species. In an earlier study in the northeastern Pacific by *Bandy et al.* [1992], no evidence of a correlation was found. Even more significant were the equatorial Pacific DMS-SO_2 shipboard observations reported during The Soviet American Gases and Aerosols (SAGA) 3 [*Huebert et al.,* 1993] and the Marine Aerosol and Gas Exchange (MAGE) [*Yvon et al., 1996b*] field studies. In the *Huebert et al.* study no causal relationship was found; whereas, in *Yvon's* and co-workers field study only upon combining five days of data in 3 hour bins was there some evidence for a causal relationship between DMS and SO_2. Yet, given that DMS typically has a lifetime of 1-2 days, that SO_2 is a major product formed from DMS oxidation, and that SO_2 from non-marine sources is small compared to that from DMS, one would clearly expect these two species to exhibit a significant anticorrelation each and every day.

Although very little "direct" evidence has been forthcoming supporting the notion that DMS oxidation gives rise to significant production of SO_2, considerable indirect evidence has been compiled that does seem to support this hypothesis. Much of this relates to aerosol observations at remote sites. Aerosol samples collected at remote marine sites have been found to contain significant levels of non-sea-salt sulfate (NSS) as well as the DMS oxidation product methane sulfonate (MS) [e.g., *Ayers and Gras*, 1991; *Ayers et al.*, 1991; *Berresheim,* 1987; *Prospero et al.*, 1991; *Saltzman et al.*, 1983, 1986; *Savoie et al.*, 1993; *Savoie and Prospero, 1989; Hertel et al.*, 1994]. These results have revealed significant correlations between MS and NSS, particularly for locations and times of the year when independent observations have revealed elevated levels of DMS to be present. The acceptance of a coupling between DMS and MS, as well as DMS and NSS, has even reached the point that the ratio of MS/NSS has been used to evaluate the relative contributions of DMS to the non-sea-salt sulfate (NSS) loading in the atmosphere. While such evaluations have proven to be quite useful, several significant issues remain unanswered as related to defining these ratios. Among these is the aerosol lifetime. Aerosol lifetimes are a strong function of both aerosol size and precipitation rates, leading to values that range from hours up to as much as a month. Furthermore, evidence exists that MS and NSS are not distributed over a similar size range of aerosols [e.g., *Huebert et al.*, 1996b, and references therein]. All this would suggest that microphysical and dynamical properties of the atmosphere could potentially have a significant impact on the measured ratio of MS and NSS at a given site. Even more important is the question of whether we actually understand the detailed chemical mechanistic processes that control the ratio of MS to NSS when the source is only DMS oxidation. Specifically, how dependent is this ratio on other environmental factors, such as temperature, humidity, aerosol surface area, NO, and HO_x radical levels. In the case of MS, although identified as a major product in laboratory chamber studies, the yields have been shown to be highly variable, depending on both the chemical mix of the chamber as well as the chamber type [*Berresheim et al.*, 1995, and references therein].

Although the early detailed kinetic study of the OH/DMS system by *Hynes et al.* [1986] provided some significant insight into the DMS oxidation process, new studies continue to reveal that this system is quite complex and far from being well understood in terms of elementary reaction processes [e.g., *Tyndall and Ravishankara*, 1989; *Barnes et al.*, 1989, 1994; *Domine et al.*, 1990; *Turnipseed and Ravishankara*,1993; *Turnipseed et al.*, 1992, 1996; *Atkinson et al.*, 1992; *Stickel et al.*, 1992; *Hynes et al.*, 1993; *Wallington et al.*, 1993; *Zhao et al.*, 1996]. In the frequently cited study by *Hynes et al.* [1986], the OH/DMS reaction was shown to proceed by both addition and abstraction pathways, the addition branch having the stronger temperature dependence and being dominant at low temperatures. These results have led some investigators to suggest that the ratio of MS to NSS should increase with decreasing temperature and hence with increasing latitude (see review by *Berresheim et al.* [1995, and references therein]). This argument presupposes, however, that (1) we know that MSA is exclusively formed through the addition channel and that the temperature dependencies of all other processes leading to the formation of aerosol phase MS are well understood, and (2) that we fully understand what fraction of each OH-initiating channel is converted into SO_2 and subsequently to NSS, and that the temperature dependencies of all steps are understood. Suffice it to say, the information now available regarding these two problem areas is far from being adequate.

Given the above setting, the field data generated during NASA's Global Tropospheric Experiment (GTE) Pacific Exploratory Mission (PEM) Tropics A field program have provided an excellent opportunity to explore several key areas of uncertainty in DMS oxidation chemistry. These include (1) direct evaluation of the DMS → SO_2 conversion efficiency for the OH/DMS reaction; (2) direct evaluation of the conversion of DMS →MSA(g); (3) identification of H_2SO_4 precursor species; (4) direct evaluation of the aerosol sticking coefficient for H_2SO_4 under tropical marine conditions, and (5) the exploration of alternative mechanisms that could lead to the formation of MS and NSS. The data used in this study were predominantly those recorded during NASA's P-3B flight 7; however, data from P-3B flights 6, 10, and 11 were also

considered, as were tropical data from NASA's DC-8 flights 4 and 5.4.2.

2. Observations

Sulfur species measured during the P-3B flight program included DMS, SO_2, H_2SO_4(g), MSA(g), MS, and NSS. Still other key measurements included OH, aerosol size/number distribution, CH_3I, dew point, and temperature. DMS and SO_2 were measured using an isotopic-dilution gas-chromatography mass-spec system involving cryogenic trapping of individual samples. This system has been previously described by *Bandy et al.* [1992, 1993]. The data collection rate for the PEM-Tropics system was typically one sample/6 min and the limit-of-detection (LOD) values for DMS and SO_2 were 2 and 1 pptv, respectively. Measurements of H_2SO_4(g), MSA(g), and OH were carried out using the chemical-ionization mass spectrometry (CIMS) technique. The typical time resolution for this system was 30 s and the LOD for all three species was in the range of 1-2 x 10^5 molec/cm^3. Details concerning the latter technique have been previously reported by *Eisele and Tanner* [1991, 1993] and Tanner and Eisele [1995]. The size/number distribution of aerosols was evaluated using three different instruments. These included an ultra-fine condensation nucleus counter (UCN-TSI 3025; Dp>0.003 μm), a condensation nucleus counter (CN-TSI 3760; Dp> 0.015 μm), a scanning 17 bin differential mobility analyzer (DMA-TSI 3071; 0.02< Dp <0.5 μm), and an optical particle counter (0.148 <Dp <6 μm). A typical time resolution for independent evaluations of the total aerosol surface area was 4-5 min. Details concerning the aerosol size/number sampling have been provided by *Clarke et al.* [this issue]. Bulk aerosol chemical analyses for MS, NSS, Na^+, Cl^-, and $NH4^+$, were carried out using a 90 mm external Teflon filter sampler (Gelmanman Zefluor, 1 μm pore size). Filter samples were extracted and analyzed by ion chromatography [*Huebert et al.*, 1996a]. Also analyzed were washings of the inlet system upon which significant aerosol had deposited. Bulk aerosol sampling times ranged from 30 to 60 min. For details see *Hoell et al.* [this issue]. Concerning all other P-3B measurements, details have been provided in the PEM-Tropics "Operational Overview" by *Hoell et al* [this issue].

As noted earlier in the text, the primary focus of this study will be the HO_x/sulfur data recorded during P-3B flight 7. During this flight, sampling of both the boundary layer (BL) and buffer layer (BuL) were carried out together with one vertical profiling of the lower free troposphere, for example, 4.8 km. The authors note that throughout this text the tropospheric region spanning the top of the BL to the bottom of lower free troposphere (LFT) will be labeled the "buffer" layer, following the recent description of this layer provided by *Russell et al.* [1998].

The data recorded during P-3B flight 7 were unique relative to those recorded during other PEM-Tropics A flights in that a Lagrangian sampling strategy permitted our following/sampling of a generic air parcel over a significant fraction of a solar cycle. As shown in schematic form in Plate 1, the strategy employed involved taking advantage of the stable wind field offered by the southeastern trades. The BL flight sequence started approximately 360 km upwind of the North Pacific site of Christmas Island with the aircraft flying toward the island on a vector of ~135°. The flight path flown during this mission consisted of a set of sequential circles

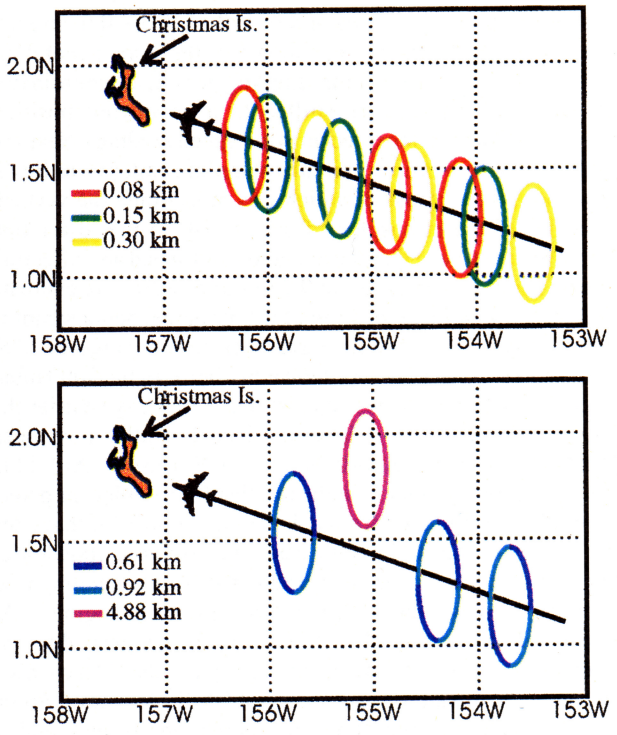

Plate 1. P-3B flight 7, Christmas Island local, August 24, 1996: Pseudo-Lagrangian flight profile. Standard altitudes are 0.075, 0.15, 0.3, 0.6, and 0.9 km.

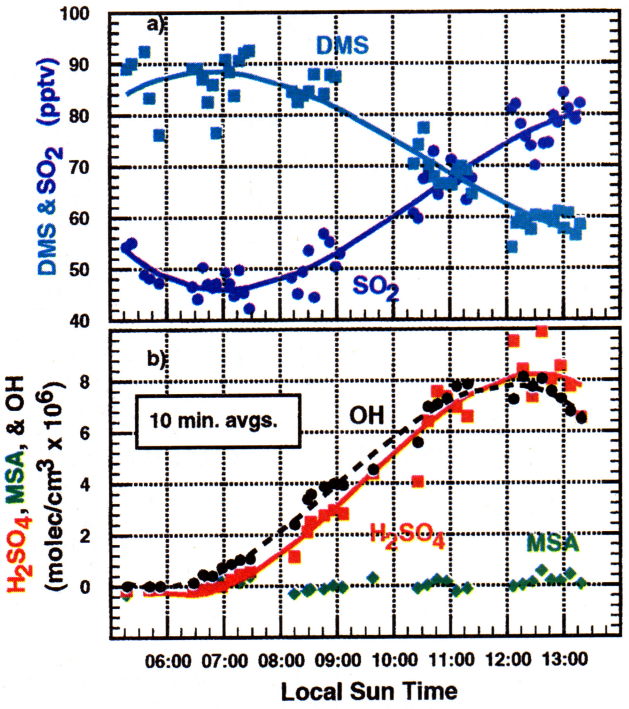

Plate 2. Diel profiles for (a) DMS and SO_2 during Christmas Island flight 7 and (b) OH, H_2SO_4, and MSA during Christmas Island flight 7. Trend lines are third-order polynomial fit.

whose altitudes were fixed at 0.075, 0.15, 0.30, 0.6, and 0.9 km. To keep the aircraft positioned in the same general air mass over the entire 8½-hour sampling period, the coordinates of each new circle were shifted to a downwind position estimated from the most recent wind speed reading. Near the midpoint of the mission, a circular sampling pattern was flown at 4.8 km, the purpose of which was to examine the vertical structure of the atmosphere from the BL to the lower free troposphere. Given that the average wind speed and direction during flight 7 were closer to 9.2 m/s and ~120°, we estimate that the geographical location of the air parcel being sampled 2 to 3 days earlier would have been in the range of 6°S, 130°W to 9°S, 137°W. As shown in Figure 1a the 1000 mbar isobaric back trajectories suggest that 2 to 3 days earlier the BL air sampled near Christmas Island would have been located between 3.5°S, 140°W and 3.5°S, 133°W. At 1.5 km (i.e., 850 mbar) Figure 1b indicates that the sampled air parcel would have originated from a location within 3° of that cited for the BL. Thus, in both cases the isobaric trajectories suggest that the air sampled originated from a geographical location well within the equatorial upwelling regime. As discussed in section 4.1, these results suggest that the "generic" air parcel followed during flight 7 should have been in contact with a significant source of DMS 2 to 3 days earlier. Further evidence supporting this contention can be found in the observations recorded during P-3B flight 11, 10 days after flight 7. Flight 11 originated from Papeete, Tahiti, and at its northern most point reached the geographical coordinates 3°S, 141°W, that is, close to the coordinates cited above for air trajectories 2 days back in time from Christmas Island. During the boundary layer run near this location, DMS levels comparable to those near Christmas Island were observed over very cold equatorial upwelling water. The estimated flux for this region was $2.6 \pm 1.5 \times 10^9$ molec/cm^2/s [G. Grodzinsky, et al.,DMS fluxes during PEM-Tropics A: Calculations based on the mass balance/photochemical model (MBPCM) approach, submitted to *Journal of Geophysical Research,* 1999], which is within 15% of that estimated near Christmas Island.

The flight 7 sulfur observational results are shown in Plates 2a and 2b. The BL data for SO_2 and DMS as a function of local sun time are those shown in Plate 2a; and those for H_2SO_4 and MSA, together with the measured level of OH, are presented in Plate 2b. The lines drawn through these data represent trend lines only (i.e., polynomial fits). Quite clearly, the results are strongly suggestive of a chemical coupling between DMS, SO_2, and OH under the tropical conditions found near Christmas Island. In particular, SO_2 clearly appears to be a major product resulting from the OH-initiated oxidation of DMS. Equally convincing is the high degree of correspondence found between SO_2, OH, and H_2SO_4(g), suggesting that the DMS oxidation product SO_2 is the dominant gas phase sulfur precursor to H_2SO_4(g) formation. By

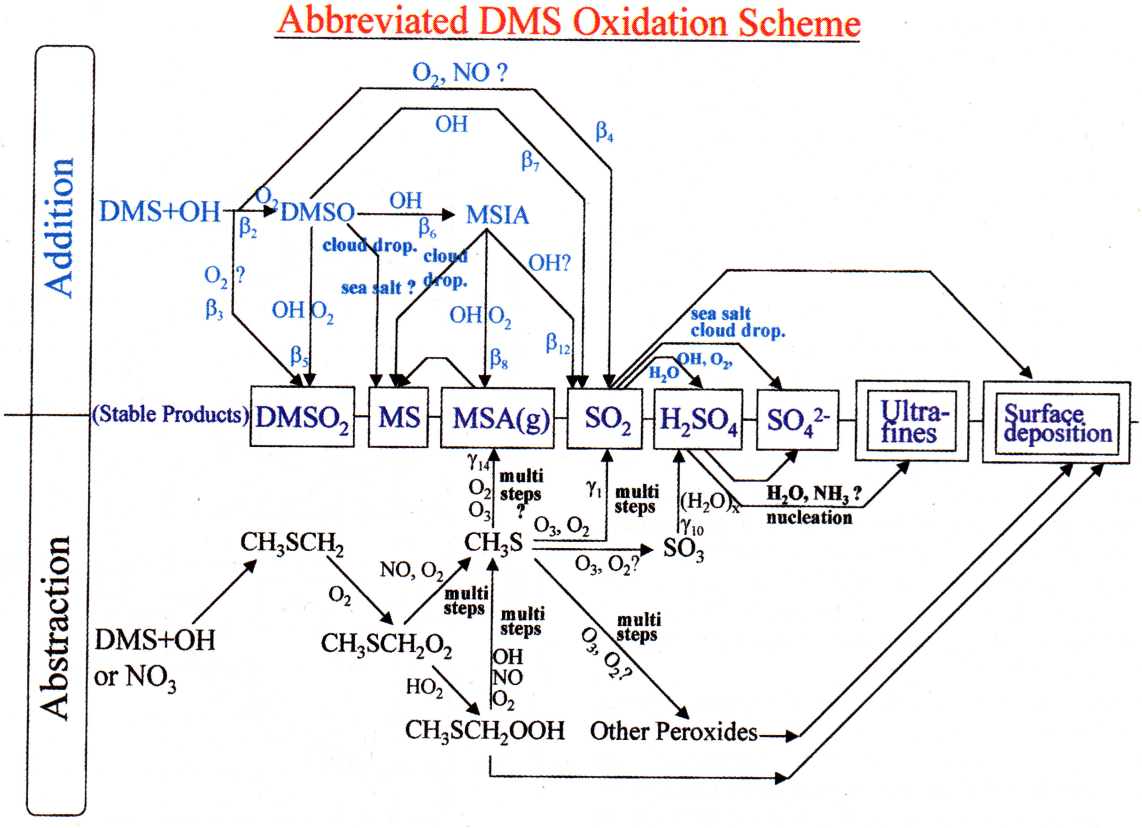

Plate 3. Abbreviated DMS oxidation scheme showing OH initiating abstraction and addition channels. The β symbols denote branching ratios for elementary reactions, and γ letters represent overall conversion efficiency factors for multistep processes. The quotation mark denotes processes for which no kinetic or field data exists to support the proposed reaction step. Chemical notation: DMSO, dimethyl sulfoxide; $DMSO_2$, dimethyl sulfone; MSIA, methane sulfinic acid; MSA(g), methanesulfonic acid; MSA(p) or MS, methane sulfonate.

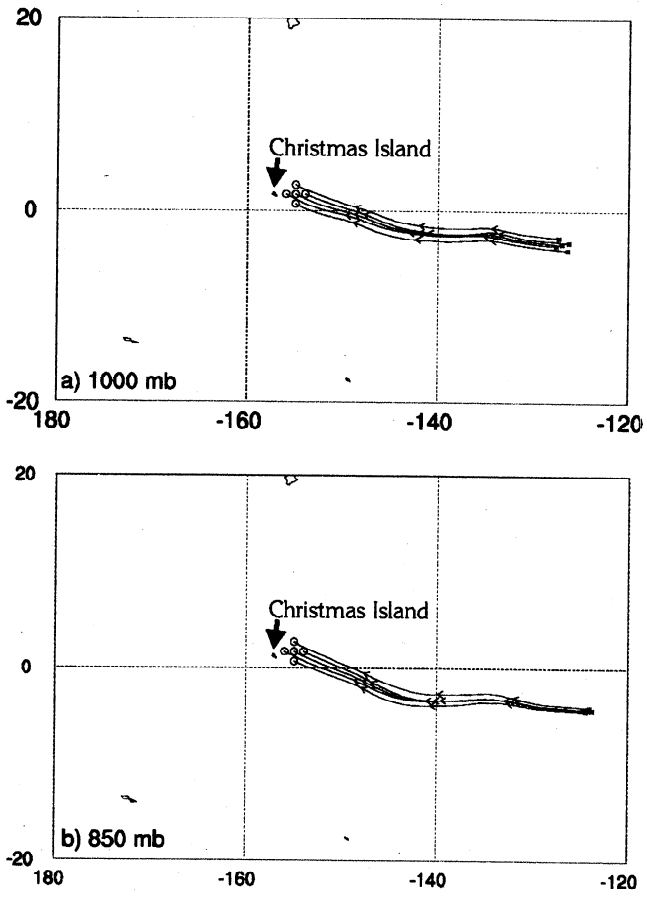

Figure 1. Four-day isobaric back trajectories arriving along the flight track of the P-3B at 1200 UTC, August 24, 1996 at a pressure altitude of: (a) 1000 mbar; and (b) 850 mbar. Circles denote arrival locations, arrows denote locations at 1 day intervals, and asterisks denote locations 4 days prior to arrival.

contrast, no clear trend is seen in MSA(g) levels as a function of solar time and/or OH levels. A detailed analysis of each of these chemical systems has been provided in sections 3.3-3.5.

3. Modeling Analysis and Discussion

3.1. Sulfur Chemistry

The salient features of the DMS oxidation chemistry used in this study are shown in Plate 3. This scheme reveals most of the key intermediates thought to be involved in the overall oxidation of DMS, the final stable end-products from this chemistry, and the critical oxidizing agents promoting this chemistry. Major uncertainties in the mechanism (e.g., steps without laboratory kinetic or field data to support them) are identified with the "?" symbol. It will also be noticed that Plate 3 contains several "β" and "γ" symbols. These symbols identify areas in the mechanism where currently it is thought that a given elementary reaction leads to more than one set of reaction products. The symbol "β" is employed to indicate a specific branching process in an elementary reaction, and thus will be refereed to as a branching ratio (BR). For cases where multi-step processes are involved in producing a stable product, with the intermediate(s) not well known or not measured, we have used the symbol "γ". Thus, γ can be viewed as an "overall conversion efficiency factor" (OCEF). In some cases it will also prove convenient to refer to not only the overall γ but to γ_{add} and γ_{abst} as they relate to product yields from specific OH reaction channels.

3.2. Detailed Model Description

Model simulations of the Christmas Island data were carried out based on a sulfur box model using 14 sulfur reactions as previously described by *D. Davis*, [1998]. Five of the 14 reactions are defined in terms of two or more branches. The respective rate coefficients, BRs, and/or OCEFs are given in tabular form in Table 1. The values cited were taken from five sources: Jet Propulsion Laboratory Publication 97-6, recent results from published laboratory kinetic studies, values estimated based on their similarity to other well studied reactions (*D. Davis, P. Wine, and M. Nikovitch*, unpublished results, 1998), estimates derived from other recent field studies [e.g., *Davis et al.*, 1998; *Bandy et al.*, 1996], and values defined in this study.

Aerosol sticking coefficients were derived from the appropriate first-order k values in conjunction with independently evaluated total aerosol surface area. The latter quantity was estimated from the measured dry aerosol size/number distribution for the size range $0.003 < Dp < 6$ μm. No aerosol data were available for estimating the surface area contributed by large sea-salt particles. However, based on other tropical aerosol field data (*A. D. Clarke*, personal communication, 1998) we have estimated that the contribution from these would have increased the reported dry surface area by not more than 20-25%. This correction was not made here since the value of this "estimated" correction was seen as modest when compared to our current estimate of the uncertainty associated with correcting the "dry surface area" values for relative humidity effects. The latter could be as large as a factor of 1.5 to 2. For flight 7, the BL and BuL relative humidity range was 73-95%. The correction for relative humidity was done using the growth profiles of *Tang* [1980]. The authors note that the uncertainty associated with the relative humidity correction to the total surface area propagates through to all estimates of the aerosol sticking coefficient, for example, $\alpha(H_2SO_4)$.

A central feature of the sulfur model used in this study is its coupling to a full $HO_x/NO_x/CH_4$/NMHC time-dependent photochemical box model constrained by measured values of NO, CO, H_2O, O_3, UV irradiance, and nonmethane hydrocarbons (when available). Details concerning the latter model have been previously described by *Davis et al.* [1993, 1996] and *Crawford et al.* [1996, 1997a,b]. Unique to this study is the fact that reasonably complete observational diel profiles of OH were available; thus, these measured values were used in our model simulations rather than calculated quantities for those time periods when available. When using J values adjusted to simulate actual solar/cloud conditions encountered during this field study, the general agreement between our model estimated OH levels and those directly measured in the field during flight 7 was typically within ± 15% *(G. Chen*, unpublished results, 1999).

Both the reaction of nighttime NO_3 and daytime OH with DMS were included in the current model mechanism; however, chlorine atom oxidation was explored as a sensitivity calculation. As related to NO_3, given the very low levels of NO_x at Christmas Island as well as for most of the tropical Pacific, the impact from NO_3 was ≤5%. The NO_x level used in this study was that reported by *J. Bradshaw et al.* [1999]

Table 1. Key Sulfur Reactions and Kinetic Parameters (T = 298 K)

No.	Reaction	Rate Coefficient and Branching Ratio
1	DMS + OH → γ_1 SO_2 +γ_{10} SO_3 + γ_{14} MSA + product	k_1(abst) = 4.2×10^{-12} cm^3/molec/s [a]; $\gamma_1 = 0.7^c$, $\gamma_{10} = 0.01^c$, $\gamma_{14} \le 0.0035^{c,h}$
2	DMS + OH→ β_2 DMSO + β_3 $DMSO_2$ + β_4 SO_2 + product	k_2(add) = 1.8×10^{-12} cm^3/molec/s[a] ; $\beta_2 = 0.8^d$, $\beta_3 = 0.0^e$, $\beta_4 = 0.2^d$, $\beta_{13} = 0.0^e$
3	DMSO + OH→β_5 $DMSO_2$ + β_6 MSIA + β_7 SO_2 + β_{13} SO_3	$k_3 = 1.0 \times 10^{-10}$ cm^3/molec/s[f]; $\beta_5 = 0.2^d$, $\beta_6 = 0.4^d$, $\beta_7 = 0.4^d$
4	MSIA + OH → β_8 MSA + β_9 H_2SO_3 + β_{12} SO_2	$k_4 = 1.0 \times 10^{-10}$ cm^3/molec/s[b]; $\beta_8 = 0.03^{c,h}$, $\beta_9 = 0.67^c$, $\beta_{12} = 0.3^e$
5	SO_2 + OH + M → HSO_3 + M	$k_5 = 8.8 \times 10^{-13}$ cm^3/molec/s[a]
6	SO_2 → dry deposition, aerosol & sea-salt scavenging	$k_6 = 1.1 \times 10^{-5}$ $1/s^{b,c,i}$
7	SO_3 + $2H_2O$ → H_2SO_4 (H_2O)	$k_7 = 2.2 \times 10^{-31}$ cm^3/molec/s[a]
8	DMSO (Heterogeneous Rx) → MS	$k_8 = 2.6 \times 10^{-4}$ $1/s^{c,j}$; $\alpha = 0.05^g$, $SA^k = 75$ $\mu m^2/cm^3$
9	MSIA (Heterogeneous Rx) → MS	$k_9 = 3.6 \times 10^{-4}$ $1/s^{e,j}$; $\alpha = 0.08^e$, $SA^k = 75$ $\mu m^2/cm^3$
10	MSA(g) → MS	$k_{10} = 3.6 \times 10^{-4}$ $1/s^c$; $\alpha = 0.08^g$, $SA^k = 75$ $\mu m^2/cm^3$
11	H_2SO_3(g) → NSS	$k_{11} = 1.3 \times 10^{-3}$ $1/s^e$; $\alpha = 0.6^e$, $SA^k = 75$ $\mu m^2/cm^3$
12	H_2SO_4(g) → NSS	$k_{12} = 1.3 \times 10^{-3}$ $1/s^c$; $\alpha = 0.6^c$, $SA^k = 75$ $\mu m^2/cm^3$
13	$DMSO_2$ → aerosol	$k_{13} = 1.5 \times 10^{-4}$ $1/s^c$; $\alpha = 0.03^g$, $SA^k = 75$ $\mu m^2/cm^3$
14	DMS + NO_3 → γ_1 SO_2 +γ_{10} SO_3 +γ_{14} MSA + product	$k_{14} = 1.0 \times 10^{-12}$ cm^3/molec/s[a]; $\gamma_1 = 0.7^{b,c}$, $\gamma_{10} = 0.01^c$, $\gamma_{14} \le 0.0035^{c,h}$

[a]De More et al., JPL 97-4 [1997].
[b]Chen et al. [J. Atmos. Chem., submitted 1999b].
[c]Estimated from this work. The authors note that the values assigned to β_9 and β_{12} could differ significantly from those given here, depending on the values assigned to β_4, β_6, and β_7.
[d]Davis et al. [1998]. See also footnote (c).
[e]Assumed value.
[f]Hynes and Wine [1996].
[g]De Bruyn et al. [1994].
[h]Overall MSA production efficiency was estimated at 0.5% from the DMS/OH addition and abstraction channels. The γ_{14} and γ_8 values were each assigned 50% of this total.
[i]This physical removal rate can be partitioned three ways: dry deposition, aerosol scavenging, and sea-alt scavenging. If dry deposition were the only pathway, the deposition velocity would be 0.6 cm/s.
[j]The rate limiting step for converting DMSO and MSIA to MSA(p) has been assigned to condensation/scavenging.
[k]SA = surface area.

since the sensor aboard the P-3B was not operational on flight 7. The *Bradshaw et al.* values were recorded during PEM-Tropics A during a Christmas Island BL flyby mission involving the NASA DC-8 aircraft. This flight took place approximately 5 days after P-3B flight 7. The NO_x levels measured at that time were approximately 10 pptv, with 3 pptv of this being NO.

In the current sulfur model, coupled sets of time-dependent continuity equations, with parameterized transport terms, are integrated to yield time dependent concentrations of sulfur species. The most general form of this equation for BL conditions is that shown below:

$$\frac{d[S]_{BL}}{dt} = \frac{F_S}{h} + \frac{M}{h}\left([S]_{BuL} - [S]_{BL}\right) + P(S) - L(S)[S]_{BL} - k_{sl}[S]_{BL} \quad (1)$$

Here $[S]_{BL}$ represents the BL concentration of the sulfur species of interest (e.g., DMS, SO_2, MSA, H_2SO_4, etc.), $[S]_{BuL}$ is the concentration of the sulfur species in the buffer layer, F_{sa} is the sea- to-air flux of S (e.g., DMS), "h" is the marine BL height, M is the mixing parameter (e.g., M=K/Δz where K is the mixing coefficient (cm^2/s) and Δz is the distance between the mid-altitude of the BL and BuL), P(S) is the photochemical production rate of sulfur species "S", L(S) is the photochemical loss of sulfur species "S", and k_{sl} is the first order physical removal rate of S via dry deposition and aerosol scavenging (dry and wet).

For most modeling runs usually one β or γ value for a key reaction or a sequence of reactions was unknown, and thus it appeared in a given calculation as an adjustable parameter. As noted earlier in the text, addressing these unknowns was one of the important objectives of this study. The approach taken in our simulations was that of defining an "acceptable range" of values for these parameters by constraining the calculation with measured sulfur concentration values. In our case, "acceptable range" was defined in terms of a chi-squared minimization fitting routine. Our "best estimate" value for the unknown parameter was then selected based on the value giving the highest level of consistency between the model-simulated curve and the sulfur observational data.

Table 2 lists the different types of simulations that were used in evaluating the flight 7 sulfur data. These have been subdivided into eight categories: (1) BL DMS/SO_2; (2) BL DMS/MSA(g); (3) BL SO_2/H_2SO_4; (4) BL SO_2/NSS; (5) BL DMSO: MSIA/MS; (6) BuL DMS/SO_2; (7) BuL SO_2/H_2SO_4; and (8) BuL DMS/MSA(g). Details concerning each type modeling run are provided in sections 3.4 -3.6.

3.3. DMS Flux Determinations

To assess the DMS flux, a mass conservation equation was employed in conjunction with measured DMS and OH values and model generated diel profiles for NO_3, e.g.,

Table 2. Summary of Model Simulation Runs

Run	
1A	BL DMS/SO_2 run, DMS/SO_2 production efficiency and SO_2 loss rate: max production efficiency.
1B	BL DMS/SO_2 run, DMS/SO_2 production efficiency: intermediate level.
1C	BL DMS/SO_2 run, DMS/SO_2 production efficiency: low level.
2A	BL DMS/MSA(g) run, DMS/MSA(g) production efficiency and surface loss characteristics: high production efficiency and normal surface loss.
2B	BL DMS/MSA(g) run, DMS/MSA(g) production efficiency and surface loss characteristics: high production efficiency and high surface loss.
2C	BL DMS/MSA(g) run, DMS/MSA(g) production efficiency and surface loss characteristics: low production efficiency and normal surface loss.
3A	BL SO_2/H_2SO_4 run, SO_2/H_2SO_4 chemical coupling.
3B	BL DMS/SO_3/H_2SO_4 run, DMS/SO_3/H_2SO_4 chemical coupling.
4A	BL SO_2/NSS via H_2SO_4 and H_2SO_3, SO_2 deposition vs. chemical conversion: no deposition.
4B	BL SO_2/NSS via H_2SO_4 and H_2SO_3, SO_2 deposition vs. chemical conversion: low deposition rate.
4C	BL SO_2/NSS via H_2SO_4 and H_2SO_3, SO_2 deposition vs. chemical conversion: intermediate deposition rate.
4D	BL SO_2/NSS via H_2SO_4 and H_2SO_3, SO_2 deposition vs. chemical conversion: no SO_2 chemical conversion.
5A	BL MS via DMSO and MSIA, MS production vs DMS/DMSO BR: high β_2.
5B	BL MS via DMSO and MSIA, MS production vs DMS/DMSO BR: intermediate β_2.
5C	BL MS via DMSO and MSIA, MS production vs DMS/DMSO BR: low β_2.
6A	BuL DMS/SO_2 run, SO_2 loss via dry deposition and aerosol scavenging: $\tau(SO_2)$ = 7 day.
6B	BuL DMS/SO_2 run, SO_2 loss via dry deposition and aerosol scavenging: $\tau(SO_2)$ = 3 day.
6C	BuL DMS/SO_2 run, SO_2 loss via dry deposition and aerosol scavenging: $\tau(SO_2)$ = 1 day.
6D	BuL DMS/SO_2 run, SO_2 loss via dry deposition and aerosol scavenging: $\tau(SO_2)$ = 0.5 day.
7A	BuL SO_2/H_2SO_4 run, SO_2/H_2SO_4 chemical coupling.
7B	BuL DMS/MSA(g) run, DMS/MSA(g) chemical coupling.

$$\frac{d[DMS]}{dt} = \frac{F_{DMS}}{EMD} - \left(k_{OH}[OH] + k_{NO_3}[NO_3]\right)[DMS] - \int_{h_{BL}}^{h_{BuL}} w\left(\frac{\partial[DMS(z)]}{\partial z}\right)dz \quad (2)$$

The formulation given in equation (2) is similar to that adopted by *Thompson et al.* [1993], *Ayers et al.* [1995], and *Yvon et al.* [1996a], with two significant adjustments. In the new formulation the BL height, "h" is replaced with the new quantity equivalent mixing depth (EMD) (see discussion below); and, in addition, a new transport term has been added to address the issue related to the influence of large scale mean vertical motion on the estimated flux. The value of the latter term is only finite for altitudes between the top of the buffer layer and top of the BL since (∂[DMS(z)]/∂z) is very close to zero for a well mixed BL. The first term on the right-hand side of equation (2) represents the DMS source term (sea-to-air flux); whereas, the second term defines the DMS chemical loss and is made up of photochemical oxidation of DMS by OH and NO_3. Based on equation (2), if the DMS mixing ratio is known at an inflection point where d[DMS]/dt = 0 and the values of EMD, [OH], [NO_3] and "w" are available, the DMS flux F_{DMS} can be solved for directly. More typical, however, is a setting where F_{DMS} is assessed through the direct comparison of model and observed DMS profiles, given that values for EMD, [OH], [NO_3], and "w" are again available. In the latter case, the value of F_{DMS} is adjusted until the difference between model-estimated and observed DMS profiles is minimized based on a chi-squared test.

The new quantity EMD can be numerically evaluated via equation (3):

$$EMD = \frac{1}{[DMS]_{BL}} \int [DMS(z)]dz \quad (3)$$

The equivalent mixing depth can thus be viewed as the height of an atmospheric column that contains all DMS mass (both buffer and boundary layers) but at BL concentrations.

As discussed by *Chen et al.* [1999], the EMD resolves the sticky problem of transport between the BL and the overhead atmospheric BuL, a problem which in the past has frequently been dealt with by using an artificially high value for the BL height [*Yvon et al.*, 1996a]. The fact that the DMS lifetime is typically quite similar in both the BL and buffer layer tends to minimize any chemistry problems arising from the use of equation (3).

Operationally, the value of EMD can be directly evaluated if there are adequate airborne observations of DMS recorded during descents and ascents to and from the BL. From a practical point of view, however, such an assessment is highly dependent on the vertical resolution of the DMS measurements. For cases where it is low, we have found that high-resolution measurements of the short-lived species CH_3I can serve as a surrogate species. The major limitation in its use is that defined by the difference in the respective lifetimes of each species. For example, CH_3I lifetime is controlled by UV photolysis and typically is 2 to 3 times longer than that for DMS. The use of CH_3I measurements therefore tends to give an upper limit value for EMD. Lower limit values, on the other hand, can be defined by the simple use of the BL height itself. As shown in Figures 2a and 2b, in the current study both DMS and CH_3I were used to evaluate EMD since the DMS data sampling rate during vertical ascents and descents was quite low. For flight 7 the results were within ~30% of

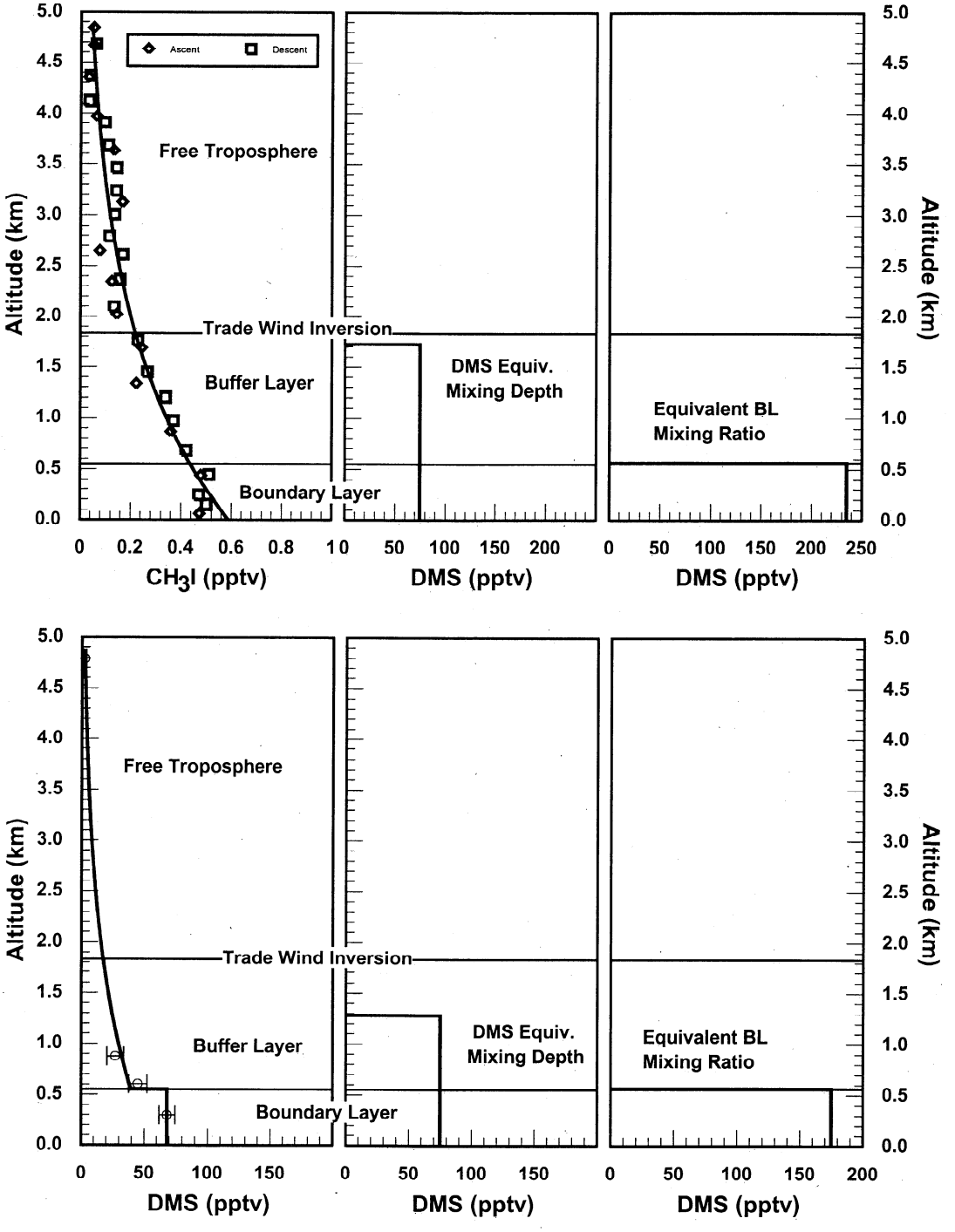

Figure 2. DMS flux assessment based on EMD as evaluated from the species (a) CH_3I and (b) DMS. P-3B flight 7, Christmas Island local, August 24, 1996.

each other, the EMD derived from DMS being 1.3 km and that from CH_3I 1.7.

From Figure 2b it can it can be seen that the mixing ratio for DMS shows a modest discontinuity at the top of the BL, followed by a near exponential roll-off moving through the BuL into the LFT. As seen in Figure 2a, no such discontinuity is observed for CH_3I, but this may partially reflect the much higher density of data for this species than for DMS. Both EMDs are seen as being significantly larger than the BL height (e.g., 0.55 km) as defined in terms of vertical plots of potential temperature and specific humidity. These results strongly suggest that either before and/or during flight 7 extensive mixing occurred between the BL and BuL, and to a more limited extent, between the BuL and LFT. To illustrate this point still further, in panel 3 of Figures 2a and 2b all DMS mass within the BL and BuL has been shifted so as to reside in the MBL (i.e., 0.55 km). The results indicate that the estimated MBL DMS mixing ratio for early morning hours

would have ranged from 230 to 175 pptv. This is 2 to 3 times higher than the maximum value observed during flight 7. These are values, however, that are actually quite similar to those reported by *Bandy et al.* [1996] during their Christmas Island ground-based sulfur study during July-August of 1994. Quite significant here is the fact that, unlike flight 7, most of *Bandy et al.'s* DMS data were collected under quiescent meteorological conditions.

On the basis of the EMD values estimated from the data shown in Figures 2a and 2b, together with flight 7 OH observational data and model-evaluated NO_3 values, estimates of the DMS flux were found to range from 2.3 to 3.0 x 10^9 molec/cm^2/s. Our "best estimate" of 2.3 ± 1.4 x 10^9 molec/cm^2/s is based on an assigned "w" value of 0.0 cm/s between 1000 and 700 mbar, as given by the NCEP mean value for the month of August 1996. Since the vertical velocity on individual days could have differed from that of the monthly mean, our best estimate flux value could still have an additional uncertainty in it beyond that cited. If, for example, a large downwelling vertical velocity had been present at the top of the BuL of 1 cm/s, the estimated flux would have increased ~30% over that cited above. *D. H. Lenschow et al.* (Use of a mixed-layer model to estimate dimethyl sulfide flux and application to other trace gas species fluxes, submitted to *Journal of Geophysical Research,* 1998), using an independent method, labeled by the authors "mixed-layer gradient method," also evaluated the DMS flux from flight 7. These authors derived a value of 6.1 ± 2.4 x 10^9 molec/cm^2/s. Although nearly two times larger, this value clearly falls within the combined uncertainties of the two independent approaches. For two other more limited DMS data sets, also recorded near Christmas Island during PEM-Tropics A (i.e., flights 6 and 10), the mass balance/photochemical approach resulted in DMS flux estimates of 3.0 ± 1.8 and 2.1±1.2 x 10^9 molec/cm^2/s, respectively. Combining the latter values with that from flight 7 gives an overall average for 3 days of sampling of 2.5 ± 1.2 x 10^9 molec/cm^2/s. This mean value can be compared to that estimated by *Bandy et al.* [1996] in their July-August 1994 Christmas Island study which resulted in a mean value of 3.7 ± 0.8 x 10^9 molec/cm^2/s. We note that Bandy et al.'s estimate was not based on photochemical modeling but rather on simple mass balance considerations. *Chen et al.* (G. Chen et al., A study of tropical DMS oxidation and DMS with model simulations, *J. Atm. Chem.*, submitted, 1999; hereafter referred to as G. Chen et al., submitted, 1999) used *Bandy et al.'s* [1994] data in conjunction with equation (2) and independently arrived at a DMS flux estimate of 3.4 ± 1.2 x 10^9 molec/cm^2/s. In Chen et al.'s assessment, as true of Bandy et al.'s, it was assumed that all DMS was in the MBL since no vertical DMS data were available. Collectively, these results suggest that the DMS flux in and around the Christmas Island region is reasonably uniform spatially and that it appears not to vary dramatically from year-to-year for non-El Niño time periods. That this should be so is perhaps not all that surprising since as noted by *Bandy et al.*, as well as other investigators [*Bates et al.*, 1992; *Huebert et al.*, 1993], Christmas Island is positioned well within the highly productive "equatorial upwelling" region of the Pacific.

3.4. DMS and SO_2 Diel Studies

As noted in section 2, although the overall flight time was weighted toward the BL (e.g., 3:1), BuL profiles were flown throughout the 8½-hour Lagrangian mission. In the text below, both atmospheric zones are investigated. The quantitative evaluation of the coupling between DMS and SO_2 was carried out using the mass balance equation (1). Its evaluation requires observational diel profiles for DMS, OH, SO_2 and NO_3. As noted earlier, the first three species were measured continuously throughout flight 7; whereas, for NO_3 only model-calculated values were available. As already discussed, however, the contribution from the NO_3/DMS reaction was found to be negligibly small, i.e., ≤3%.

The value of the mixing parameter "M" was independently evaluated using equation (1) based on a comparison of the observational DMS profile with that derived from our sulfur model. Input to the model consisted of the evaluated DMS flux F_{DMS} and the OH diel profile. Values of M were adjusted so as to minimize the chi-square value estimated from a comparison of the two curves. As shown in Figure 3, for an M value of 1.2 cm/s the model profile for DMS was found to be well within the SD (standard deviation) for the DMS observations. Taking Δz as 0.9 km resulted in an estimated value for the mixing coefficient K of ~11 m^2/s. This value appears to be consistent with the conclusion drawn earlier, based on vertical chemical profile data, which strongly suggested that the vertical distributions of the trace gas species CH_3I and DMS were significantly influenced by shallow convection.

Having assigned a value to M, a second parameter that required evaluation in the analysis of the coupling between DMS and SO_2 was the first-order SO_2 loss coefficient "k_{sl}". This "k" value incorporates deposition to the ocean's surface, scavenging by liquid and/or particulate aerosols, as well as reaction of SO_2 with sea-salt. It was assigned an initial value of 1.1 x 10^{-5} s^{-1}, based on the1994 Christmas Island data of *Bandy et al.*

Given the above values for M and k_{sl} and the diel profile for SO_2, equation (1) was used to assess the "overall/total" SO_2 conversion efficiency from DMS (e.g.,γ_{total}) as well as to estimate possible values for the abstraction channel (i.e., γ_{abst} or γ_1) and for all addition channels (γ_{add}). Recall, the contribution to SO_2 production from the addition channel is defined by contributions from three branching ratios β_4, β_7 and β_{12} (e.g., see Plate 3). As shown in Figure 3, the results indicate that the best fit to the SO_2 observational profile is realized when γ_{total} is 100%. This, of course, suggests that the values of γ_1 as well as β_4, β_7, and β_{12} are all near unity. This result is significantly higher than that estimated from the 1994 Christmas Island data recorded by *Bandy et al.* [1996]. The latter authors reported a γ_{total} value for SO_2 of 62 ± 5%. G. Chen et al. (submitted, 1999), using the same database, but using the current model, arrived at virtually the same value, i.e., 65±13%. A value of 100% is also in conflict with other field observations [e.g., *Bandy et al.*, 1996; *Huebert et al.*, 1993; *Davis et al.*, 1998] as well as chamber studies [*Barnes et al.*, 1996, *Sørensen et al.*, 1996] which collectively show that the oxidation of DMS leads to the formation of other sulfur-containing products. Included among these are DMSO, $DMSO_2$, MSIA, MSA, and MS.

To achieve a conversion efficiency similar to that reported by *Bandy et al.* [1996], the best model fit requires the lowest SO_2 profile shown in Figure 3 (e.g., curve C). For this case γ_{total} is ~0.57, which represents a deviation in the estimated and observed mixing ratios for SO_2 of nearly 24%. Given that

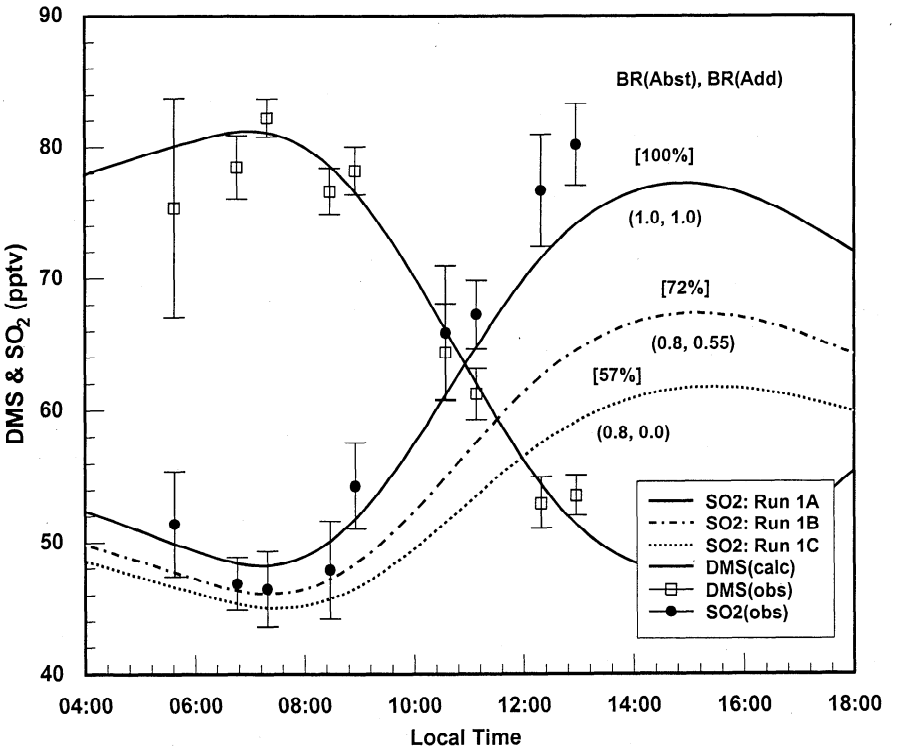

Figure 3. Observed and model-generated BL diel profiles for DMS and SO_2 (runs 1A, 1B, and 1C), P-3B flight 7. Error bars on observational data represent one standard deviation. Numbers in parenthesis are the estimated branching ratio values for the conversion of DMS to SO_2 for the OH/DMS abstraction and addition channels, respectively. Numbers in square brackets represent γ_{total} or the overall conversion efficiency of DMS to SO_2. The first-order SO_2 loss rate used in these simulations was estimated at 1.1×10^{-5} s^{-1}, based on run 1A.

nearly 70% of the OH/DMS reaction rate is defined by the abstraction channel at BL temperatures of 298 K, if all SO_2 were formed only through this channel (e.g., β_4, β_7, and β_{12} = 0.0), the value of γ_{abst} would be 0.7. For purposes of the current analysis, we have estimated that the minimal yield of other DMS oxidation products would be ~8% and have then taken the lower limit value of γ_{total} to be 52%, as suggested by *Bandy et al.* and G. Chen et al.'s (submitted, 1999) analysis of the 1994 Christmas data set. This has led to the our selection of curve B as representing the "best estimate"of the overall DMS to SO_2 conversion efficiency, i.e., 0.72 ± 0.22. Reflecting this higher γ_{total} value, we have tentatively assigned SO_2 contributions from the abstraction channel, γ_{abst} to be 0.8 and that from the addition channel, γ_{add}, of 0.6. Obviously, values as high as 1.0 could also be assigned to γ_{abst} with still lower values for γ_{add}. The values of 0.8 and 0.6 are proposed in the current study based on two other pieces of evidence. The first of these involves the recent results reported from the Antarctic Sulfur Chemistry in the Antarctic Tropospheric Experiment (SCATE) study. In contrast to the current study, ~75% of the total DMS/OH reaction rate was defined by the addition channel. Although SO_2 itself was not measured in the SCATE study, the relatively high observed levels of both H_2SO_4(g) and DMSO led *Davis et al.* [1998] to conclude that the DMS/OH addition channel was a major source of SO_2. Corroborating evidence supporting this position can be found in the results from recent chamber studies reported by *Sørensen et al.* [1996] and *Barnes et al.* [1989]. Both research groups examined the products generated from the DMSO/OH reaction. In both cases, SO_2 was found to be among the major products identified.

Although the above arguments would seem to support the notion that γ_{total} values for SO_2 formation might be expected to be closer to 0.70, the fact that the flight 7 data are most compatible with values of 1.0 leads one to conclude that there most likely are some important aspects of this field study that are still not fully understood and/or properly represented. For example, it is possible that significant inhomogeneities existed within the region sampled due to the extensive shallow convection in the area. If so, one could argue that the measured SO_2 may not have been representative. Evidence supporting this notion can be found in the sizeable variations observed in the levels of SO_2 within some of the individual BL circular sampling patterns (e.g., ± 11%).

One could also ask whether inhomogeneities in the DMS flux field may not have been the source of the problem. For example, in another related study (unpublished results), BL DMS/SO_2 exploratory modeling runs illustrated what could happen if a generic air parcel were allowed to sequentially pass over contiguous marine regions having quite different DMS flux fields. As related to flight 7, these results suggest that an elevated DMS flux field upwind of the region sampled, but still well within the equatorial up-welling, could have been a major contributor to the observed elevated levels of SO_2. In combination with the inhomogeneity issues just raised there is also the question of how well the complex transport processes

involved in the Christmas Island study were represented in our model. As noted earlier in section 3.2, vertical transport in our study was parameterized in the form of a single non-time varying value for the mixing parameter, "M". This obviously represents a significant over-simplification of the dynamical processes occurring during the Christmas Island study.

A quite different answer to the SO_2 shortfall issue could be that we simply failed to measure all available biogenic sources of sulfur, e.g., dimethyl disulfide (DMDS). Model simulations suggest that because of the large difference in the OH rate coefficients (i.e., nearly a factor of 40), only a very modest DMDS ocean flux (i.e., 10 times smaller than that for DMS) would be adequate to get closure on SO_2. At these low flux levels, no significant early morning perturbation occurs in the model-generated SO_2 profile. As of this writing, however, no investigator has reported a measurable flux for this species, reflecting in no small part the difficulty of making reliable measurements of this sulfur compound.

Still a final possibility for explaining a possible shortfall in SO_2 sources might involve the role of halogen chemistry. Chlorine atoms are known to react with DMS at gas kinetic collision rates, forming yet another pathway to SO_2 [*Stickel et al.*, 1992]. Over the last 10 years, several investigators have hypothesized the possible importance of this marine chemistry. Mechanisms put forward to explain the presence of reactive chlorine typically involve its formation by heterogeneous sea-salt reactions [e.g., *Keene et al.*, 1990; *Singh and Kasting*, 1988; *Pszenny et al.*, 1993; *Singh et al.*, 1996a; and *Wingenter et al.*, 1996]. We have tested this possibility here in model simulations which have assumed a constant reactive chlorine (e.g., Cl_2 or HOCl) flux throughout the day, thus resulting in a substantial buildup of labile chlorine under dark conditions. In these model runs the addition of reactive chlorine led to a very large enhancement in the photochemical production of Cl atoms at sunrise which necessarily permitted our upping our projected DMS flux. The magnitude of this new flux was limited by the shifts occurring in the concentration profiles of both DMS and SO_2. Using a chi-squared test as an indicator of the "goodness-of-fit," we estimated the increase in the DMS flux that could be tolerated without causing a substantial reduction in the agreement between model and observational profiles. The results showed that DMS flux increases of only 10% could be justified. This level of enhancement resulted in only a 7% increase in the SO_2 max value. Using the much more extensive 1994 Christmas Island data of *Bandy et al.*, a similar analysis resulted in a slightly lower limit for the influence of halogen chemistry, e.g., 5-10% (G. Chen et al., submitted 1999). Both results appear to be consistent with the recent findings of *Singh et al.* [1996b], who used atmospheric budget arguments involving the species C_2Cl_4 to show that the contribution from Cl oxidation of DMS may not be much greater than ~3%.

While the reactive chlorine and DMDS hypotheses represent potential new sources of SO_2 in the marine BL, it is far more difficult to extend each of these arguments to the BuL. Because of its greater separation from sources of both sea-salt and surface-released DMDS, one would expect BuL SO_2 contributions from these sources to be even smaller than for the MBL. The observations, however, show the SO_2 modeled shortfall to be even larger than that for the BL. For example, from Figure 4 SO_2 levels are seen as equal to or even slightly larger than those observed in the BL for similar times

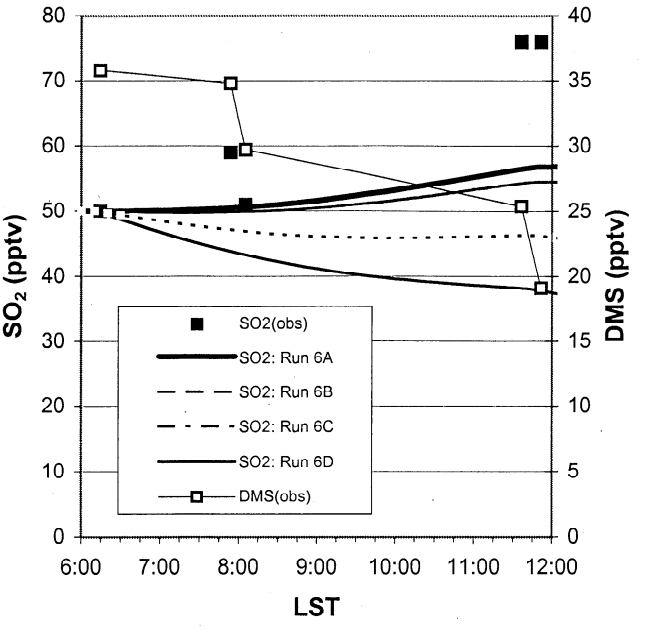

Figure 4. Observed and model generated BuL diel profiles for DMS and SO_2 (runs 6A, 6B, 6C, and 6D), P-3B flight 7. BR_{abst} DMS/OH/SO_2) = 0.8, BR_{add} (DMS/OH/SO_2) = 0.2, BR_{add} (DMSO/OH/SO_2) = 0.4; model run 6A: $\tau(SO_2)$ = 7 days; model run 6B: $\tau(SO_2)$ = 3 days; model run 6C: $\tau(SO_2)$ = 1 day; model run 6D: $\tau(SO_2)$ = 0.5 days.

of day. However, because of lower DMS levels, the model simulations predict SO_2 levels that are only 50% of the values observed. Even when making the assumption that all DMS was converted to SO_2 with 100% efficiency and that SO_2 had an extended lifetime at higher altitudes (e.g., 7 days), only 70% of the observed SO_2 could be accounted for. The possibility that SO_2 might have been transported into the BuL from the LFT must also be considered; but the observations at 4.5 km revealing SO_2 levels of no more than 30 pptv would seem to preclude the importance of this source.

As in the case of the BL, therefore, we have concluded that the apparent SO_2 shortfall predicted by the model for the BuL is probably attributable to a combination of factors. These most likely involve nonrepresentative sampling of the region as well as limitations on the current model's ability to handle the complex transport processes occurring immediately before and during flight 7.

3.5. SO_2 and H_2SO_4 Diel Studies

One of the critical questions raised in several earlier studies on the oxidation of DMS is that of identifying the most important chemical pathway by which H_2SO_4(g) is formed [*Bandy et al.*, 1992; *Lin and Chameides*, 1993]. Two of the most frequently cited paths are summarized below and involve the direct formation from DMS of either the intermediate SO_3 or SO_2:

(R1a) DMS + OH → (multisteps) → SO_3 + other products

(R2a) $SO_3 + 2H_2O \rightarrow H_2SO_4(g)$

(R1b) DMS + OH → (multisteps) → SO_2 + other products

(R2b) $SO_2 + OH + M \rightarrow HOSO_2 + M$

(R3b) $HOSO_2 + O_2 \rightarrow SO_3 + HO_2$

The flight 7 data permit an indirect assessment of γ_{10}, the OCEF that defines how much SO_3 is formed via the multistep process (R1a). Note that when SO_3 is formed, it is quickly converted to H_2SO_4(g) via the highly efficient reaction (R2a). Recent kinetic studies have shown that this process proceeds in two steps, involving a quadratic dependence on H_2O [*Lovejoy et al.*, 1996; *Molina*, private communication, 1998]. Given the great abundance of H_2O in the MBL, this typically results in a lifetime for SO_3 that is less than a few minutes.

To be examined here is whether the flight 7 SO_2 and OH profiles are consistent with the simultaneously recorded H_2SO_4(g) profile. If so, one could infer that the value of γ_{10} would necessarily have to be quite small. Recall, in our previous discussions of SO_2 it was concluded that free tropospheric sources of this species were not important and that oxidation of DMS was the dominant BL source of this sulfur species. Given these conditions and the reaction sequence R1a → R3b, the formation of H_2SO_4(g) from DMS photochemical sources can be expressed in terms of equation (4):

$$P(H_2SO_4)_{DMS} = k_{2b}[SO_2]_{DMS}[OH][M] + k_{2a}[SO_3]_{DMS}[H_2O]^2 \quad (4)$$

Here $[SO_2]_{DMS}$ can be equated to $[SO_2]_{obs}$; whereas $[SO_3]_{DMS}$, based on abstraction being the only source of SO_3 formation, can be defined as:

$$[SO_3]_{DMS} = \frac{\gamma_{10} k_{abs(1a)}[DMS][OH]}{k_{2a}[H_2O]^2} \quad (5)$$

Given the rate coefficient for reaction (2b) and the diel profiles for SO_2 and OH, equation (1) can be used to solve for the concentration levels of H_2SO_4(g) provided both γ_{10} and the first-order loss for H_2SO_4 $k_{sl}(H_2SO_4)$ are assigned values. (Note, loss of H_2SO_4 via nucleation processes has not been considered here since the level of ultra-fine particles measured was quite low, and the total aerosol surface area was quite large.) In Plate 4 we show the calculated level of H_2SO_4(g) for the case where the value of γ_{10} has been assumed to be zero. Thus, only the SO_2/OH reaction is involved in H_2SO_4(g) formation; and the numerical value of $k_{sl}(H_2SO_4)$ therefore can be evaluated directly from the observed H_2SO_4(g) profile. In our case, the resulting $k_{sl}(H_2SO_4)$ value was determined to be 1.3 x 10^{-3} s^{-1}. More importantly, from Plate 4 it is quite apparent that these results are consistent with the notion that H_2SO_4(g) is a product of the reaction sequence (1b), (2b), and (3b), followed by (2a). Taking still a different approach to testing this agreement, we independently evaluated the quantity $k_{sl}(H_2SO_4)$ using the measured total aerosol surface area (corrected for relative humidity) together with the recent laboratory measured value (i.e., 0.75) for the H_2SO_4 sticking coefficient [*Jefferson et al.*, 1997]. In this case the model calculated value of H_2SO_4 was still found to be within 15% of the observed. Using the same assumptions and an adjusted value for $k_{sl}(H_2SO_4)$, similar good agreement was also found for the BuL as shown in Figure 5.

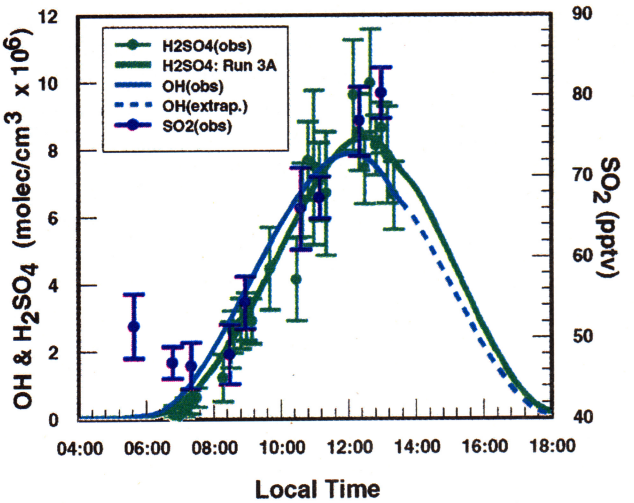

Plate 4. Observed and model-generated BL diel profiles for H_2SO_4 based on observed OH, and SO_2 (run 3A), P-3B flight 7. Error bars on observational data represent one standard deviation, blocked integration time for OH and H_2SO_4 is 10 min. Estimated particle surface area equal to 75 $\mu m^2/cm^3$, $k_{sl}(H_2SO_4) = 1.3 \times 10^{-3}$ s^{-1}.

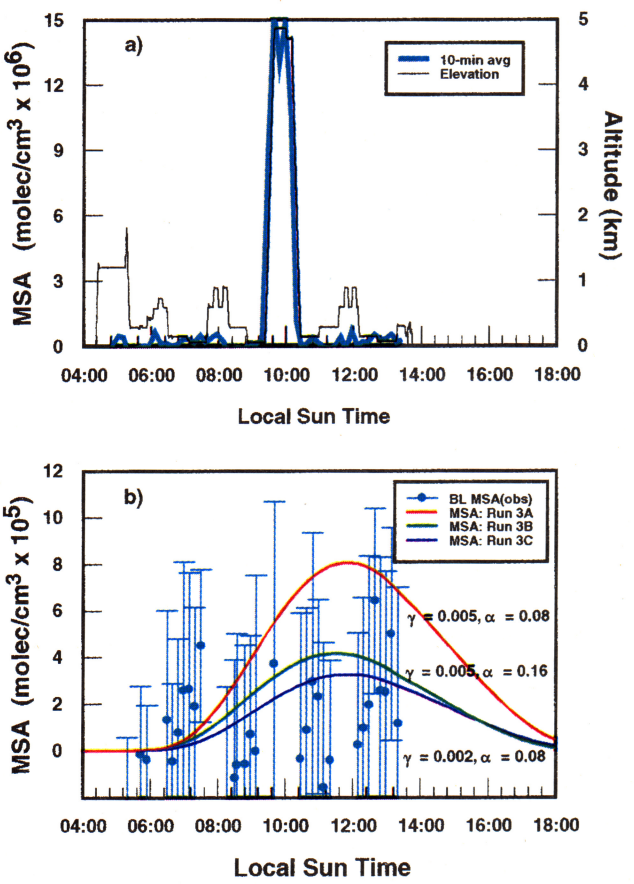

Plate 5. (a) Time line plots of altitude and observed MSA(g), P-3B flight 7. (b) Observed and model-generated BL diel profiles for MSA(g) (runs 2A, 2B, and 2C), P-3B flight 7. Estimated particle surface area equal to 75 $\mu m^2/cm^3$, α (MSA) = 0.08 ([De Bruyn *et al.*, 1994], and τ(MSA) = 43 min. Negative values for MSA(g) indicate the level of noise in the measurements, e.g., 1-2 x 10^5 molecules/cm^3.

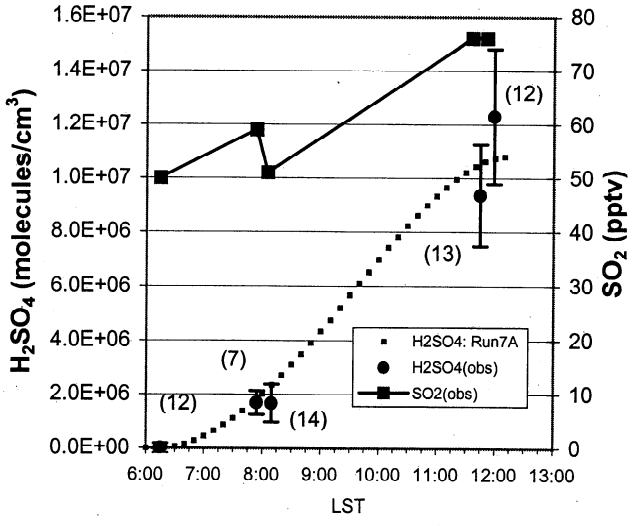

Figure 5. Observed and model-generated BuL diel profiles for H_2SO_4 (run 7A), P-3B flight 7. Estimated particle surface area equal to 50 $\mu m^2/cm^3$; $k_{sl}(H_2SO_4) = 0.85 \times 10^{-3}$ s^{-1}.

Although the SO_2 precursor pathway looks quite promising, one can still raise the question whether an equally satisfactory answer could not be found by assuming a rather large value for γ_{10}. For example, if the value of γ_{10} were ~0.5, model simulations predict that the SO_3 formation pathway would be the dominant source of H_2SO_4(g), e.g., ~85%. However, if true, this would also suggest that for any given observational time period the quantity k_1[OH][DMS] would be strongly correlated with the actual observed H_2SO_4(g) level (see reaction list in Table 1.). One would predict, in fact, that the latter correlation should exceed that for the alternate pathway, k_5[OH][SO_2][M], since the lifetime of SO_2 is much longer than that for SO_3 and H_2SO_4. As shown in Figures 6a and 6b, this is not found to be the case. A simple regression analysis of k_1[OH][DMS] versus [H_2SO_4(g)] produces an R^2 value of 0.81; whereas, k_5[OH][SO_2][M] versus [H_2SO_4(g)] gives an R^2 value of 0.97. In this case, since k_1[OH][DMS] is also the major source of SO_2, it follows that a significant correlation should be present relative to H_2SO_4 even if the production of SO_3 were negligibly small. Quite interestingly, if only those data are used that were recorded after 1100 hrs local sun time (i.e., the time period for maximum H_2SO_4 production), the R^2 value for k_1[OH][DMS] versus [H_2SO_4(g)] drops to less than 0.1. By contrast, for k_5[OH][SO_2][M] versus [H_2SO_4(g)] the correlation weakens, as expected due to the much smaller dynamic range of values, but drops to only 0.41, suggesting once again that the SO_3 channel is most likely a very minor one. A similar conclusion was reached by *Davis et al.* [1998] and *Jefferson et al.* [1998] in their independent analysis of the H_2SO_4(g) field data recorded during the Antarctic SCATE program.

On the basis of an evaluated "wet" aerosol total surface area of 75 $\mu m^2/cm^3$, our previously estimated "best-fit" value for the first-order loss of H_2SO_4 (e.g., $k_{sl}(H_2SO_4) = 1.3 \times 10^{-3}$ s^{-1}) makes possible an independent evaluation of the critically important H_2SO_4 sticking coefficient α. For flight 7 the value derived for the MBL was 0.6 ± 0.3. A similar analysis, but involving data from the BuL (i.e., surface area = 50 $\mu m^2/cm^3$), led to an $\alpha(H_2SO_4)$ value of 0.55 ± 0.30. Both results are in quite good agreement with the laboratory study by *Jefferson et al.* [1997], (e.g., 0.76± 0.20) using polydispersed aerosol at a relative humidity of ≤20%. Our evaluations were based on use of the *Fuchs and Sutugin* [1970] equation as integrated over the flight 7 measured aerosol size/# distributions. In this assessment we assumed that loss of H_2SO_4 via dry deposition was negligible. The major uncertainties associated with the current work would appear to involve the reliability of the conversion of the measured dry aerosol size distribution to a wet one involving very high relative humidities. In our case, this conversion was carried out in a similar fashion as that described by *Clarke et. al.* [1996a]. The uncertainty factor assigned to this conversion is estimated to be as high as ±1.5. Evaluation of the H_2SO_4 diffusivity for BL conditions was based on a hydrated H_2SO_4 molecule involving 1.9 water molecules [*R. Weber*, Private communication].

3.6. MSA Diel Studies

As shown in Plate 3, gas phase MSA is a possible product from both the OH/DMS addition and abstraction channels.

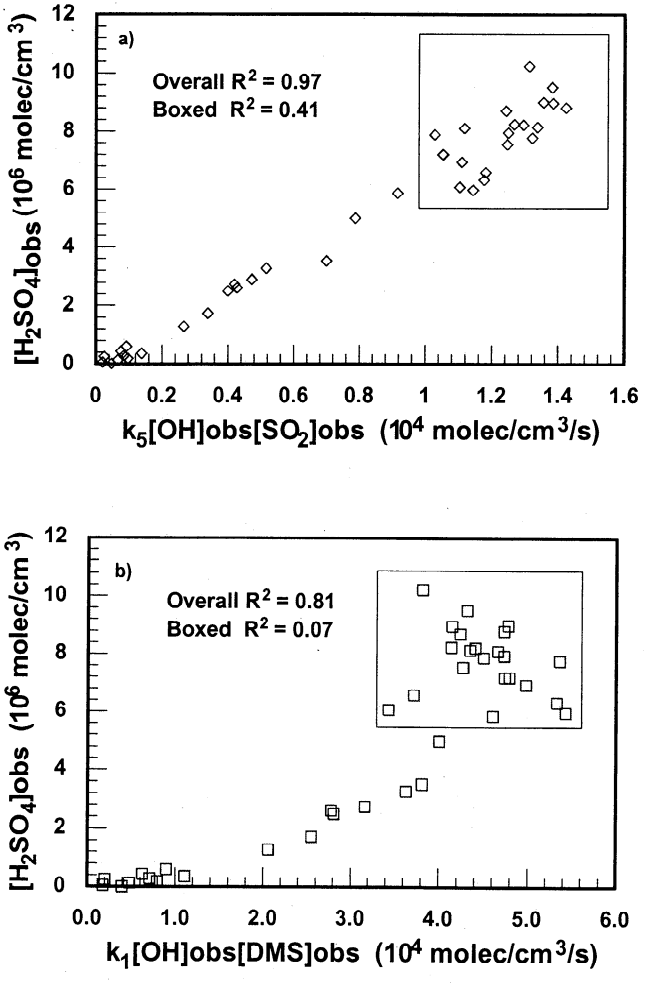

Figure 6. Correlation plot of $[H_2SO_4]_{obs}$ versus (a) $k_5[OH]_{obs}$ $[SO_2]_{obs}$ and (b) $k_1[OH]_{obs}$ $[DMS]_{obs}$. Data enclosed in box were recorded between 1100 and 1330 hrs local sun time.

Suffice it to say, no chamber or detailed kinetic study has quantitatively answered this important question even though quite frequently it is assumed that only the addition channel contributes to MSA formation. In the very recently reported SCATE sulfur field study, *Davis et al.* [1998] found that the diel profiles of MSA were consistent with an addition channel source; however, they could not rule out contributions from the much smaller OH/DMS abstraction channel.

The flight 7 MSA(g) observations are shown in Plate 5a. Quite interesting here is the large variation seen in the levels of MSA(g) as a function of altitude, for example, over 2 orders of magnitude. Most evident from these data is the fact that the highest values of MSA are those associated with the highest altitudes (1.5 x 10^7 molecules/cm^3). By contrast, BL values are typically seen as approaching the LOD. of the CIMS instrument (e.g., 1-2 x 10^5 molecules/cm^3). In Plate 5b, greater detail is provided concerning the range of MSA(g) values observed during the BL sampling portions of flight 7. Also given are the results from three model simulations. These simulations were based on three different combinations of the values for the parameters γ_{MSA} (defined in terms of γ_{14}, β_2, β_6, and β_8) and α(MSA). Quite apparent here is the fact that the value of γ_{MSA} is surprisingly small, i.e., less than 1%. Since nearly 70% of the OH/DMS reaction proceeds through the abstraction channel, these results would tend to argue that the abstraction channel is most likely a very weak and perhaps nonexistent source of MSA(g). Equally important, they strongly suggest that the overall production of gas phase MSA is totally incapable of explaining the much larger observed level of BL MS of 15.1 pptv, even assuming that the average lifetimes for MBL aerosols is of the order of 2 to 4 days. Similar MSA(g) yields (e.g., averaging 1-2%) were found for several other tropical BL flights, both during PEM-Tropics A as well as during the First Aerosol Characterization Experiment (ACE-1) field program (*D. Davis*, unpublished results, 1998).

As shown in Figure 7, the high noon BuL MSA results are about a factor of 2.5 times higher than those observed in the BL; however, even these values are seen as being inconsistent with the adjusted MSA(g) loss rate and the value for k(DMS/OH-addition). The dramatic increase in MSA(g) seen at 4.5 km most likely reflects a still further complexity of the MSA system, for example, the likelihood of an equilibrium between MSA(g) and MSA(aerosol) [*Mauldin et al.*, this issue] with this equilibrium being highly dependent on relative humidity.

4. Sulfur Budget Assessment

4.1. MSA(g) and MS Budget

As cited in the above text, the very low yield of gas phase MSA was found to be too small to explain observed BL levels of MS. It follows that these low yields could not be the basis for the frequently cited tropical value for the ratio MS/NSS of 7 to 9% [e.g., *Savoie and Prosper*, 1989; *Saltzman et al.*, 1983, 1986; *Bates et al.*, 1992; *Huebert et al.*, 1993]. In fact, for PEM-Tropics A P-3B flight 7, the value of this ratio was also found to be near 8%. This raises a very interesting question: What is the missing source of particulate MS?

In the case of flight 7, the possibility that MS could be transported from the BuL seems quite unlikely. As indicated in Figure 8, MS levels in this zone were 2 to 3 times lower than for the BL. From Figure 7 it is also apparent that the BuL source strength of gas phase MSA is far too small. Yet another possibility would be in-cloud oxidation of DMS as recently proposed by Lee and Zhou [1994]. In their mechanism the scavenging of both O_3 and DMS by cloud droplets leads to an aqueous phase reaction with a rate coefficient at 15°C of 4 × 10^8 $M^{-1}s^{-1}$. The product from this reaction has been reported to be DMSO. As discussed later in the text, further reaction of DMSO in the aqueous phase could hypothetically provide the necessary source of MS. Lee and Zhou have provided an initial assessment of the chemical consequences of this DMS/O_3 in-cloud chemistry in that they have shown that it could remove/oxidize an amount of DMS comparable to that assigned to OH given that the diel averaged value for OH were 1 × 10^6 molec./cm^3, the liquid water concentration was 1 g/m^3, and the O_3 level was 30 ppbv. A careful examination of the marine BL conditions presented during flight 7, however, would seem to suggest otherwise. In fact, an inspection of each critical factor involved would place the liquid phase DMS oxidation rate closer to 20 times lower than that for removal via reaction with OH. The basis for this revised factor lies in: 1) the diel OH level being 2 times higher for flight 7, 2) the O_3 level being 2.5 times lower in flight 7, and 3) the cloud liquid water concentration during flight 7 being a factor of 4 lower. Thus, our current assessment is that the liquid phase DMS/O_3 reaction is not a major factor in the bulk removal/oxidation of DMS in the marine BL. Even so, this does not preclude the possibility that the liquid phase oxidation of DMS, producing liquid phase DMSO, may still have made a modest contribution to the level of MS in the aerosol phase.

We propose here that the major source of MS was provided by heterogeneous processes involving the gas phase DMS oxidation products DMSO (dimethyl sulfoxide) and MSIA (methane sulfinic acid). *Jefferson et al.* [1998] have previously suggested the gas phase DMSO source as a way of

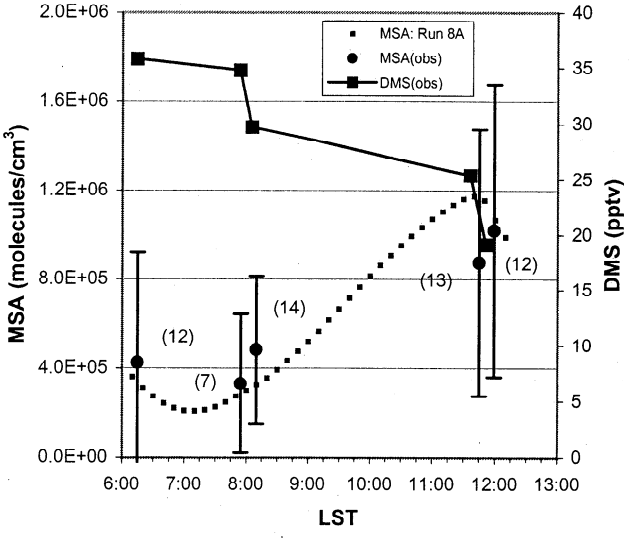

Figure 7. Observed and model-generated BuL diel profiles for MSA(g) (run 8A), P-3B flight 7. Estimated particle surface area equal to 50 $\mu m^2/cm^3$, α (MSA) = 0.08 [*De Bruyn et al.*, 1994], and τ(MSA) = 66 min.

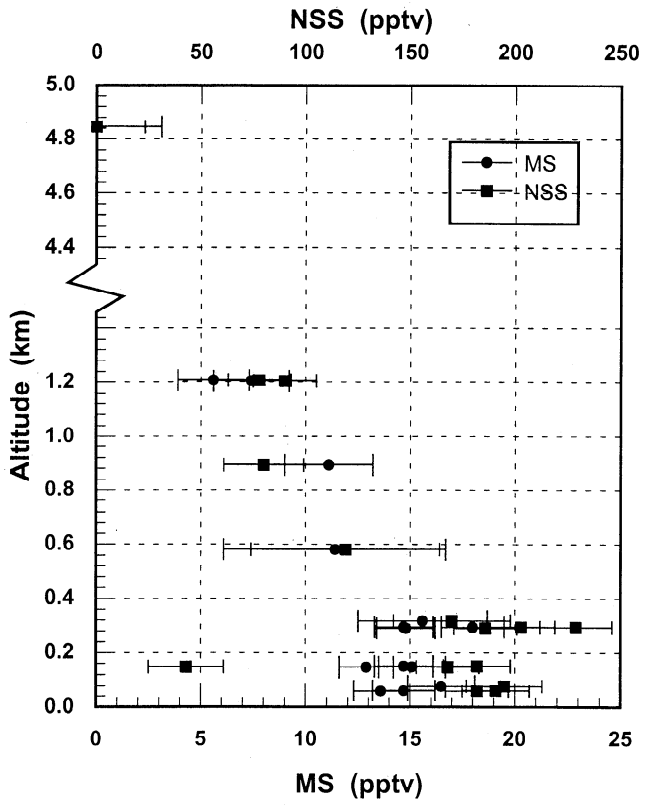

Figure 8. Vertical profiles of Methane Sulfonate (MS) and non-sea-salt sulfate (NSS). Solid squares denote NSS, and solid circles denote MS. Error bars represent one standard deviation.

explaining the high levels of MS observed during the Antarctic project SCATE. These authors noted that liquid-phase laboratory-kinetic studies have demonstrated that DMSO in aqueous solution is readily oxidized by OH to form MSIA which, in turn, is found to be further oxidized to form MS [*Schested and Holeman*, 1996; *Scaduto*, 1995; *Veltwisch et al.*, 1980]. Although not measured during PEM-Tropics, average mixing ratios of DMSO of 2.5 pptv, with spike values as high as 25 pptv, were reported during the Antarctic field program SCATE [*Davis et al.*, 1998; *Berresheim et al.*, 1998]. *Bandy et al.* [1996] also reported observing significant levels of DMSO in their 1994 Christmas Island study. Finally, both DMSO and MSIA have been reported as products in recent DMS/OH chamber studies [*Sørensen et al.*,1996; *Barnes et al.*, 1996].

To evaluate the heterogeneous chemical hypothesis for the flight 7 data, model simulations were carried out using the abbreviated chemical scheme summarized in Plate 3. Thus time-dependent profiles of DMSO were generated with the major loss of this species being to aerosols. The sticking coefficient adopted for this simulation was that reported by *De Bruyn et al.* [1994], e.g., 0.05. The results are those shown in Table 3a. From here it can be seen that, using the recently estimated value for β_2 of 0.8 (*Davis et al.* [1998]), a 2.5 day aerosol lifetime, and the above-cited *De Bruyn et al.* α(DMSO) value, sufficient DMSO and MSIA are produced from the gas phase oxidation of DMS to explain 100% of the observed BL MS loading of 15.1± 1.4 pptv. Although encouraging, it is recognized that this estimate is critically dependent on the exact value chosen for β_2. If, for example, the value of β_2 were decreased to 0.5 or 0.2, the average lifetime required for MS aerosols would necessarily be extended to 4 and 10 days, respectively. Current estimates for 1 μm or smaller marine aerosols are in the 3-7 day range [see *Warneck*, 1988, and references therein]. Thus, if the value of β_2 were to be as small as 0.2, even the heterogeneous pathway would not be adequate to explain the observed MS loading. In summary, though still speculative in nature, the DMSO and MSIA heterogeneous pathways appear quite promising as a major source of MS.

4.2. NSS Budget

Model simulation results addressing the issue of NSS sources are shown in Table 3b. A critical quantity that required specification in these runs was the loss of SO_2 to the ocean's surface versus its removal by heterogeneous oxidation to sulfate. The latter can occur on particulate aerosols and/or within cloud droplets. Literature values for surface deposition range from 0.2 to 0.7 cm/s [*Sheih et al.*, 1979, and references therein]. However, the most appropriate value to use in any given application obviously depends on the actual environmental setting. At present, there is no widely accepted quantitative relation from which to compute its value. Current thinking is that as much as half probably goes to the ocean's surface, but much uncertainty exists in these estimates.

For flight 7, even though at the time of the flight the marine BL had approximately 20-30% cloud coverage, it is still quite difficult to sort out the earlier history of the air parcel within which much of the NSS formation could have occurred. Most likely both cloud processing as well as heterogeneous reactions on sea-salt aerosols contributed to the production of NSS during flight 7 [*Hegg*, 1985, 1990; *Chameides and Stelson*, 1992; *Sievering et al.*, 1992, 1995]. Given this starting condition, we have presented in Table 3b two different scenarios for the partitioning of SO_2 between ocean surface deposition, formation of H_2SO_4 via reaction with OH, and heterogeneous conversion to sulfate. In each of these, H_2SO_4 production has been constrained by observational data, as has the total amount of NSS.

In scenario 1 an SO_2 deposition velocity of 0.15 cm/s is assumed which, to satisfy the BL NSS observation of 190 ± 18 pptv, requires a BL aerosol lifetime of 3.4 days. (The authors note that the focus in this assessment is primarily on aerosol ≤1 μm since current information suggest that 85 to 95% of the NSS is on particles of this size range [e.g., *Huebert et al.*, 1993, 1996a; *Sievering et al.*, 1990; *Pszenny et al.*, 1990]). Scenario 1 suggests that ~33% of the DMS-generated SO_2 is deposited to the ocean's surface; and of the NSS observed, heterogeneous conversion of SO_2 would define 78% of the total. The remainder of the NSS would primarily be defined by condensation of gas phase H_2SO_4. For scenario 2 a deposition velocity of 0.45 cm/s is used, the required aerosol lifetime being 7.1 days. Under these conditions, nearly 65% of the SO_2 is shunted to the ocean's surface, and heterogeneous conversion of SO_2 to NSS defines only 54% of the total.

Given the results of Tables 3a and 3b, together with the independent determinations of the aerosol lifetime at Christmas Island based on the 1994 study (i.e., 2-4 days) [*Huebert et al.*, 1996a; *Clarke et al.*, 1996b], we estimate that

Table 3a. BL Production of MS From DMSO, MSIA, and MSA(g) as a Function of the Branching Ratio β_2

β_2	MS Lifetime Needed[a]	Source Species	Calculated MS pptv	Percent Contribution
0.8	2.5 day	DMSO[b]	11.5	76
		MSIA[b]	3.4	23
		MSA(g)[c]	0.2	1
Total			15.1	100
0.5	4.0 day	DMSO[b]	11.4	75
		MSIA[b]	3.4	23
		MSA(g)[c]	0.3	2
Total			15.1	100
0.2	9.7 day	DMSO[b]	11.0	73
		MSIA[b]	3.3	22
		MSA(g)[c]	0.8	5
Total			15.1	100
Observed MS = 15.1 ± 1.4 pptv				

[a] Lifetime needed to reproduce MS from gas phase sources.
[b] Model predictions.
[c] Model calculation constrained by observations.

the ocean surface deposition velocity for SO_2 most likely falls into the range of 0.15 to 0.30 cm/s. However, it must be emphasized that this result is critically dependent on the reported measurement of NSS being representative of the equatorial region sampled. If, for example, the NSS level were three times lower, the deposition velocity range estimated would be increased by nearly a factor of three. Quite interestingly, the above-cited deposition range of 0.15 to 0.30 cm/s also appears to be compatible with the independent results calculated by *D. Davis* (unpublished results), who analyzed the marine sulfur data from Lagrangian flight sequence B of the ACE-1 field program. He was able to derive an internally consistent sulfur budget when using an average SO_2 deposition velocity of ~0.3 cm/s. For illustration purposes, we have selected an intermediate value from the cited range of deposition velocities (e.g., 0.25 cm/s). For this specific case the ultimate fate of the photochemically generated tropical BL SO_2 would consist of: (1) ~39% would be deposited to the ocean's surface; (2) 46% would be converted to NSS via various forms of heterogeneous reactions, including cloud processes; and, (3) ~15% would be converted to gas phase H_2SO_4, nearly all of which would be subsequently scavenged to form NSS. These results can be contrasted to those of *Yvon et al.* [1996b], also recorded in the tropical Pacific, which suggested that ~58% of the SO_2 was deposited to the ocean, 37% was converted to NSS via heterogeneous processes, and 5% was oxidized by OH to form H_2SO_4. Thus, the general level of agreement is quite good.

An interesting quantity that can be extracted from the flight 7 breakout is what may be labeled "the bulk rate of

Table 3b. BL Production of NSS From H_2SO_4, H_2SO_3,, and SO_2 as a Function of the SO_2 Deposition Velocity

$Vd(SO_2)$ cm/s	NSS Lifetime Needed[a]	Source Species	Calculated NSS pptv	Percent Contribution
0.15	3.4 day	H_2SO_4(g)[b]	35	18
		H_2SO_3(g)[c]	7	4
		SO_2[b]	148	78
Total			190	100
0.45	7.1 day	H_2SO_4(g)[b]	74	39
		H_2SO_3(g)[c]	14	7
		SO_2[b]	102	54
Total			190	100

[a] Lifetime needed to reproduce NSS from gas phase sources.
[b] Model calculated diurnal averages constrained by observations.
[c] Model predicated diurnal averages.

production" of BL NSS from SO_2 heterogeneous processes. For example, given a diurnal average value for SO_2 of 60 pptv, this rate would be estimated at 1.0×10^4 molec/cm^3/s. For comparison purposes, the average value calculated from 10 days of sampling during the 1994 Christmas Island study has been evaluated at 1.6×10^4 molec/cm^3/s. Future aerosol studies hopefully will provide still further points of comparison for a much wider range of atmospheric conditions.

5. Summary and Conclusions

The diel profile data from the PEM-Tropics flight 7 Christmas Island study have convincingly demonstrated that SO_2 is a major product from the OH/DMS oxidation process. Furthermore, all evidence points to DMS being the dominant source of SO_2 in this environment. Our best estimate for the overall SO_2 conversion efficiency γ_{total} is ~72%, although some evidence suggests that it could be higher. The above cited SO_2 yield from DMS is most consistent with both the OH/DMS abstraction and addition branches contributing to the production of SO_2. At the high temperatures of the tropical BL, abstraction provides the largest contribution with our best estimate of γ_1 being ~0.8. Contributions from chlorine atom oxidation chemistry appear to be no larger than 5 to 10% of that for OH for the tropical conditions encountered at Christmas Island.

An internally consistent picture involving SO_2 and NSS was developed for the Christmas Island study which revealed that over half of the photochemically produced SO_2 is converted to NSS. This appears to occur through both the formation of gas phase H_2SO_4 (15%), followed by condensation, and from heterogeneous processes (46%). This suggests that perhaps 39% of the SO_2 is deposited directly to the ocean surface, resulting in an estimated deposition velocity for SO_2 of ~0.25 cm/s. Both of the latter values, however, could be as much as a factor of 2 higher, depending upon the representativeness of the NSS observations.

Using as input to the model measured values for SO_2 and OH, the level of agreement between observed and model simulated BL H_2SO_4(g) profiles was found to be exceptionally good. These results, in conjunction with correlation analyses, suggest that for the tropical conditions near Christmas Island the dominant sulfur precursor in the formation of H_2SO_4 is SO_2 rather than the more speculative species SO_3, e.g., $\gamma_{10} \approx 0.0$. Using the observed H_2SO_4 diel profile, the model estimated H_2SO_4 formation rate, and the total aerosol surface area, the H_2SO_4 sticking coefficient α was evaluated at 0.6 ± 0.3. A similar value was determined for the BuL. These high values suggests that H_2SO_4 molecules are removed with very high efficiency upon collision with sea-salt particles.

Taking the observed NSS and MS levels at Christmas Island to be representative of the region, these data strongly suggest that both the levels of NSS and MS are predominantly controlled by heterogeneous processes for a tropical BL setting. In the case of MS, model simulations suggest that the DMS oxidation products DMSO and MSIA are most likely the key species involved. Gas phase production of MSA was shown to account for only ~1% of the observed MS. By contrast, gas phase production of H_2SO_4 (and perhaps H_2SO_3) appears to account for ~20% of the NSS, leaving ~80% of the NSS having as its source various forms of heterogeneous reactions, including in-cloud processes.

Our conclusions concerning the sources of MS and NSS are of particular significance in that BL measured values of the ratio MS/NSS have often been used to estimate the fraction of NSS derived from biogenic DMS. It also has been used at times to infer the temperature environment under which DMS oxidation occurred. The primarily assumption that must be made in each case is that the rates for the initiating OH abstraction and addition reactions dictate the product distribution. Critical to the effective use of this ratio, however, is having a very clear understanding of what the actual oxidation products are at a given temperature. Equally important is having a good understanding of what the rate controlling step(s) is/(are) for each product. In some cases the rate of the initiating reaction involving OH probably does provide a reasonable basis for interpreting the MS/NSS ratio. However, for many environments it would seem that this interpretation could be quite problematic.

In a marine tropical environment, for example, our results suggest that the final value for this ratio is strongly predicated on BL heterogeneous chemistry. However, the heterogeneous processes involved in forming MS and NSS may have different temperature dependencies, and quite possibly are influenced to different degrees by the availability of oxidizing agents on aerosol surfaces or levels of oxidants in the aqueous phase. Additionally, one cannot be completely sure at this point whether the critical rate-determining step(s) are gas phase or heterogeneous processes. In the case of heterogeneous conversions involving surfaces, typically the gas transfer rate to the surface itself is rate determining; by contrast, for short-lived liquid aerosols, processes within the aqueous phase can be controlling.

Equally challenging to our old ideas of DMS oxidation is the fact that the product SO_2 now appears to be formed both from the OH addition as well as abstraction channels. Thus, a decrease in temperature, which might have been viewed as causing a decrease in the yield of SO_2 from the abstraction channel, might actually be compensated for by new production from the addition channel. As noted earlier in the text, the latter channel is known to have a strong negative temperature dependency. It is possible, therefore, that the rate of SO_2 production (for a given level of DMS) might even increase with decreasing temperatures. Similarly, DMSO, which under tropical BL conditions appears to be the major source of MS via heterogeneous reactions, could behave chemically quite differently if formed under low-temperature and low-aerosol conditions. For example, instead of being lost to aerosol surfaces, we would predict that it would react with OH to produce SO_2, MSIA, MSA, or possibly other products.

In spite of these unresolved issues, we believe the current study has enhanced our understanding concerning the factors controlling the distribution of DMS oxidation products. However, many new questions have been raised and some old questions still remain unanswered. New field studies which measure a wider range of DMS oxidation products (e.g., DMSO and $DMSO_2$) over a 24-hour cycle will be essential. In addition, detailed laboratory kinetic studies of both gas phase and heterogeneous processes will be needed.

Acknowledgment. This work was supported in part by funds from the National Aeronautics and Space Administration under grants NAG-1-1769 and NAG 1-1766. D. D. Davis would also like to thank the project office at NASA Langley Research Center and the flight crews at NASA Wallops Island for their dedicated support of the PEM-Tropics program.

References

Andreae, M. O., and W. R. Barnard, The marine chemistry of dimethylsulfide, *Mari. Chem.*, *14*, 267-269, 1984.

Andreae, M. O., and H. Raemdonck, Dimethyl sulfide in the surface ocean and the marine atmosphere: A global view, *Science*, *221*, 744-747, 1983.

Andreae, M. O., R. J. Ferek, F. Bermond, K. P. Byrd, R. T. Engstrom, S. Hardin, P. D. Houmere, F. LeMarrec, H. Raemdonck, and R. B. Chatfield, Dimethyl sulfide in the marine atmosphere, *J. Geophys. Res.*, *90*, 12,891-12,900, 1985.

Atkinson, R., D. L. Baulch, R. A. Cox, R. F. Hampson Jr., J.A. Kerr, and J. Troe, Evaluated kinetic and photochemical data for atmospheric chemistry, Supplement IV, IUPAC subcommittee on gas kinetic data evaluation for atmospheric chemistry, *J. Phys. Chem. Ref. Data, 21,* 1125-1568, 1992.

Ayers, G. P., and J. L. Gras, Seasonal relationship between cloud condensation nuclei and aerosol methanesulfonate in marine air, *Nature, 353,* 834-835, 1991.

Ayers, G. P., Ivey, J. P., and R. W. Gillett, Coherence between seasonal cycles of dimethyl sulphide, methanesulphonate, and sulphate in marine air, *Nature, 349,* 404-406, 1991.

Bandy, A. R., D. L. Scott, B. W. Blomquist, S. W. Chen, and D. C. Thornton, Low yields of SO_2 from dimethyl sulfide oxidation in the marine boundary layer, *Geophys. Res. Lett., 19,* 1125-1127, 1992.

Bandy, A. R., D. C. Thornton, A. R. Driedger III, Airborne measurements of sulfur dioxide, dimethyl sulfide, carbon disulfide, and carbonyl sulfide by isotope dilution gas chromatography/mass spectrometry, *J. Geophys. Res., 98,* 23,423, 1993.

Bandy, A. R., D. C. Thornton, B. W. Blomquist, S. Chen, T. P. Wade, J. C. Ianni, G. M. Mitchell, and W. Nadler, Chemistry of dimethyl sulfide in the equatorial Pacific atmosphere, *Geophys. Res. Lett.*, *23*, 741-744, 1996.

Barnes, I., V. Bastain, K. H. Becker, and D. Martin, Fourier Transform IR studies of the reactions of dimethyl sulfoxide with OH, NO_3, and Cl radicals, in *Biogenic Sulfur in the Environment*, edited by E. S. Saltzman and W. J. Cooper, *Am. Chem. Soc.*, Washington, D. C., 1989.

Barnes, I., K.H. Becker, and I. Patroescu, The tropospheric oxidation of dimethyl sulfide: A new source of carbonyl sulfide, *Geophys. Res. Lett.*, *21,* 2389-2392, 1994.

Barnes, I., K. H. Becker, and I. Patroescu, FTIR product study of the OH initiated oxidation of dimethyl sulphide: Observation of carbonyl sulphide and dimethyl sulphoxide, *Atmos. Environ.*, *30,* 1805-1814, 1996.

Bates, T. S., B. K. Lamb, A. Guenther, J. Dignon, R. E. and Stoiber, Sulfur emissions to the atmosphere from natural sources, *J. Atmos. Chem.*, *14*, 315-337, 1992.

Berresheim, H., Biogenic sulfur emissions from the Subantarctic and Antarctic Oceans, *J. Geophys. Res.*, *92,* 13,245-13,262, 1987.

Berresheim, H., P. Wine, and D. Davis, Sulfur in the atmosphere, in *Composition, Chemistry, and Climate of the Atmosphere,* edited by H. B. Singh, pp. 251-307, Van Nostrand Reinhold, New York, 1995.

Berresheim, H., J. W. Huey, R. P. Thorn, F. L. Eisele, D. J. Tanner, and A. Jefferson, Measurements of dimethylsulfide, dimethylsulfoxide, dimethylsulfone, and aerosol ions at Palmer Station, Antarctica, *J. Geophys. Res.*, *103*, 1629-1637, 1998.

Bradshaw, J., D. Davis, J. Crawford,G. Chen, R. Shetter, M. Muller, G. Gregory, G. Sachse, D. Blake, B. Heikes, H. Singh, J. Mastramarino, and S. Sandholm, Photofragmentation two-photon laser-induced fluoresence detection of NO_2 and NO: Comparison of measurements with model results based on airborne observations during PEM-Tropics A, *Geophys. Res. Lett.*, in press, 1999.

Chameides, W. L., and A. W. Stelson, Aqueous-phase chemical processes in deliquescent sea-salt aerosols: A mechanism that couples the atmospheric cycles of S and sea-salt, *J. Geophys. Res.*, *97*, 20,565-20,580, 1992.

Chen, G., D. Davis, P. Kasibhatla, A. Bandy, and D. Thornton, A mass balance/photochemical assessment of DMS sea-to-air flux as inferred from NASA GTE PEM-West A and B observations, *J. Geophys. Res.*, in press, 1999.

Clarke, A. D., J. N. Porter, F. Valero and P. Pillewski, Vertical profiles, aerosol microphysics and optical closure during ASTEX: Measured and modeled column optical properties, *J. Geophys. Res., 101,* 4443-4453, 1996a.

Clarke, A.D., Z. Li, and M. Litchy, Aerosol dynamics in the equatorial Pacific marine boundary layer: Microphysics, diurnal cycles, and entrainment, *Geophys. Res. Lett., 23*, 733-736, 1996b.

Clarke, A. D., F. Eisele, V. N. Kapustin, K. Moore, R. Tanner, L. Mauldin, M. Litchy, B. Lienert, M. A. Carroll, and G. Albercook, Nucleation in the equatorial free troposphere: Favorable environments during PEM-Tropics, *J. Geophys. Res.*, this issue.

Crawford, J. H., et al., Photostationary state analysis of the NO_2-NO system based on airborne observations from the western and central North Pacific, *J. Geophys. Res., 101*, 2053-2072, 1996.

Crawford, J. H., et al., Implications of large scale shifts in tropospheric NO_x levels in the remote tropical Pacific, *J. Geophys. Res.*, *102,* 28,447-28,468, 1997a.

Crawford, J. H., et al., An assessment of ozone photochemistry in the extratropical western North Pacific: Impact of continental outflow during the late winter/earlier spring, *J. Geophys. Res., 102*, 28,469-28,487, 1997b.

Davis, D. D., et al., Photostationary state analysis of the NO_2-NO system based on airborne observations from the subtropical/tropical North and South Atlantic, *J. Geophys. Res., 98,* 23,501-23,523, 1993.

Davis, D. D., et al., Assessment of the ozone photochemistry tendency in the western North Pacific as inferred from PEM-West A observations during the fall of 1991, *J. Geophys. Res., 101*, 2111-2134, 1996.

Davis, D. D., G. Chen, P. Kasibhatla, A. Jefferson, D. Tanner, F. Eisele, D. Lenschow, W. Neff, and H. Berresheim, DMS oxidation in the Antarctic marine boundary layer: Comparison of model simulations and field observations of DMS, DMSO, DM SO_2, H_2SO_4 (g), MSA(g), and MSA(p), *J. Geophys. Res.*, *103,* 1657-1678, 1998.

De Bruyn, W. J., J. A. Shorter, P. Davidovits, D. R. Worsnop, M. S. Zahniser, and C. E. Kolb, Uptake of gas phase sulfur species methanesulfonic acid, dimethylsulfoxide, and dimethyl sulfone by aqueous surfaces, *J. Geophys. Res., 99,* 16,927-16,932, 1994.

Domine, F., T. P. Murrells, and C. J. Howard, Kinetics of the reactions of NO_2 with CH_3 S, CH_3 SO, CH_3 SS, and CH_3SSO at 297 K and 1 torr, *J. Phys. Chem., 94,* 5839-5847, 1990.

Edwards, A. L., *Multiple Regression and Analysis of Variance and Covariance,* W. H. Freeman, New York, 1985.

Eisele, F. L., and D. J. Tanner, Ion assisted tropospheric OH measurement, *J. Geophys. Res., 96,* 9295, 1991.

Eisele, F. L., and D. J. Tanner, Measurement of the gas phase concentration of H_2SO_4 and methane sulfonic acid and estimates of H_2SO_4 production and loss in the atmosphere, *J. Geophys. Res., 98,* 9001, 1993.

Fuchs, N.A., and A.G. Sutugin, Highly Dispersed Aerosols, Ann Arbor Science Publishers, Ann Arbor, Michigan, 1970.

Grosjean, D., Photooxidation of methyl sulfide, ethyl sulfide, and methanethiol, *Environ. Sci. Technol, 18,* 460-468, 1984.

Hatakeyama, S., K. Izumi, and H. Akimoto, Yield of SO_2 and formation of aerosol in the photo-oxidation of DMS under atmospheric conditions, *Atmos. Environ., 19,* 135-141, 1985.

Hegg, D. A., The importance of liquid-phase oxidation of SO_2 in the troposphere, *J. Geophys. Res., 90,* 3773-3779, 1985.

Hegg, D. A., Heterogeneous production of cloud condensation nuclei in the marine atmospheres. *Geophys. Res. Lett., 17,* 2165-2168, 1990.

Hertel, O., J. Christensen, and Ø. Hov, Modelling of the end products of the chemical decomposition of DMS in the marine boundary layer, *Atmos. Environ., 28*, 2431-2449, 1994.

Hoell, J., et al., Pacific Exploratory Mission in the Tropical Pacific: PEM-Tropics A, August-September 1996, *J. Geophys. Res.*, this issue.

Huebert, B. J., S. Howell, P. Laj, J. E. Johnson, T. S. Bates, P. K. Quinn, V. Yegorov, A. D. Clarke, and J. N. Porter, Observations of the atmospheric sulfur cycle on SAGA-3, *J. Geophys. Res., 98,* 16,985-16,996, 1993.

Huebert, B. J., L. Zhuang, S. Howell, K. Noone, and B. Noone, Sulfate, nitrate, methanesulfonate, chloride, ammonium, and sodium measurements from ship, island, and aircraft during ASTEX/MAGE, *J. Geophys. Res., 101*, 4413-4423, 1996a.

Huebert, B. J., D. J. Wylie, L. Zhuang, and J. A. Heath, Production

and loss of methanesulfonic and non-sea-salt sulfate in the equatorial Pacific marine boundary layer, *Geophys. Res. Lett., 23,* 737-740, 1996b.

Hynes, A. J., P. H. Wine, and D. H. Semmes, Kinetics and mechanism of OH reactions with organic sulfides, *J. Phys. Chem., 90,* 4148-4156, 1986.

Hynes, A. J., R. E. Stickel, A. J. Pounds, Z. Zhao, T. McKay, J. D. Bradshaw, and P. H. Wine, Mechanistic studies of the OH-induced oxidation of dimethylsulfide, in *Proceedings of the International Symposium on Dimethylsulfide: Oceans, Atmosphere, and Climate,* pp. 211-221, edited by G. Restelli and G. Angeletti, Kluwer Acad., Norwell, Mass., 1993.

Jefferson, A., F. L. Eisele, P. J. Ziemann, R. J. Weber, J. J. Marti, and P. H. McMurry, Measurements of the H_2SO_4 mass accommodation coefficient onto polydisperse aerosol, *J. Geophys. Res., 102,* 19,021-19,028, 1997.

Jefferson, A., D. J. Tanner, F. L. Eisele, J. W. Huey, D. D. Davis, G. Chen, A. Torres, and H. Berresheim, OH oxidation chemistry and MSA formation in the coastal Antarctic boundary layer, *J. Geophys. Res., 103,* 1647-1656, 1998.

Keene, W. C., A. A. P. Pszenny, D. J. Jacob, R. A. Duce, J. N. Galloway, J. J. Schultz-Tokos, H. Sievering, and J. F. Boatman, The geochemical cycling of reactive chlorine through the marine troposphere, *Global Biogeochem. Cycles, 4,* 407-430, 1990.

Lee, Yin-Nan and Xianliang Zhou, Aqueous reaction kinetics of ozone and dimethylsulfide and its atmospheric implications, *J. Geophys. Res., 99,* 3,597-3,605, 1994.

Lin, X., and W. L. Chameides, CCN formation from DMS oxidation without SO_2 acting as an intermediate, *Geophys. Res. Lett., 20,* 579-582, 1993.

Lovejoy, E. R., D. R. Hanson, and L. G. Huey, Kinetics and products of the gas-phase reaction of SO_3 with water, *J. Phys. Chem., 100,* 19,911-19,916, 1996.

Lovelock, J. E., R. J. Maggs, and R. A. Rasmussen, Atmospheric dimethyl sulphide and the natural sulphur cycle, *Nature, 237,* 462-463, 1972.

Mauldin, R. L. III, D. J. Tanner, J. A. Heath, B. J. Huebert, and F. L. Eisele, Observations of H_2SO_4 and MSA during PEM-Tropics, *J. Geophys. Res.*, this issue.

Niki, H., P. D. Maker, C. M. Savage, and L. P. Breitenbach, An FTIR study of the mechanism for the reaction HO + CH_3SCH_3, *Int. J. Chem. Kinet., 15,* 647-654, 1983.

Prospero, J. M., D. L. Savoie, E. S. Saltzman, and R. Larsen, Impact of oceanic sources of biogenic sulphur on sulphate aerosol concentrations at Mawson, Antarctica, *Nature, 350,* 221- 223, 1991.

Pszenny, A. P., G. R. Harvey, C. J. Brown, R. F. Lang, W. C. Keene, J. N. Galloway, and J. T. Merrill, Measurements of dimethyl sulfide oxidation products in the summertime North Atlantic marine boundary layer, *Global Biogeochem. Cycles, 4,* 367-379, 1990.

Pszenny, A. A. P., W. C. Keene, D. J. Jacob, S. Fan, J. R. Maben, M. P. Zetwo, M. Springer-Young, and J. N. Galloway, Evidence of inorganic chlorine gases other than hydrogen chloride in marine surface air, *Geophys. Res. Lett., 20,* 699-702, 1993.

Russell, L. M., D. H. Lenschow, K. K. Laursen, T. S. Bates, A. R. Bandy, and D. Thornton, Bidirectional mixing in an ACE-1 marine boundary layer overlain by a second turbulent layer, *J. Geophys. Res., 103,* 16,411-16,432, 1998.

Saltzman, E. S., D. L. Savoie, R. G. Zika, and J. M. Prospero, Methane sulfonic acid in the marine atmosphere, *J. Geophys. Res., 88,* 10,897-10,902, 1983.

Saltzman, E. S., D. L. Savoie, J. M. Prospero, and R. G. Zika, Methanesulfonic acid and non-sea-salt sulfate in Pacific air: Regional and seasonal variations, *J. Atmos. Chem., 4,* 227-240, 1986.

Savoie, D. L., and J. M. Prospero, Comparison of oceanic and continental sources of non-sea-salt sulphate over the Pacific Ocean, *Nature, 339,* 685-687, 1989.

Savoie, D. L., J. M. Prospero, R. J. Larsen, F. Huang, M. A. Izaguirre, T. Huang, T. H. Snowdon, L. Custals, and C. G. Sanderson, Nitrogen and sulfur species in Antarctic aerosols at Mawson, Palmer Station, and Marsh (King George Island), *J. Atmos. Chem., 17,* 95-122, 1993.

Scaduto, R. C., Oxidation of DMSO and methanesulfinic acid by the hydroxyl radical, *Free Radical Biol. Medi., 18,* 271-277, 1995.

Schested, K., and J. Holeman, A pulse radiolysis study of the OH radical induced autooxidation of methanesulfinic acid, *Radiat. Phys. Chem., 3,* 357-360, 1996.

Sheih, C. M., M. L. Wesely, and B. B. Hicks, Estimated dry deposition velocities of sulfur over the eastern United States and surrounding regions, *Atmos. Environ., 13,* 1361-1368, 1979.

Sievering, H., G. Ennis, and E. Gorman, Size distributions and statistical analysis on nitrate, excess sulfate, and chloride deficit in the marine boundary layer during the GCE/CASE/WATOX, *Global Biogeochem. Cycles, 4,* 395-405, 1990.

Sievering, H., J. Boatman, E. Gorman, Y. Kim, L. Anderson, G. Ennis, M. Luria, and S. Pandis, Removal of sulphur from the marine boundary layer by ozone oxidation in sea-salt aerosol, *Nature, 360,* 571-573, 1992.

Sievering, H., E. Gorman, T. Ley, A. Pszenny, M. Springer-Young, J. Boatman, Y. Kim, C. Nagamoto, and D. Wellman, Ozone oxidation of sulfur in sea-salt aerosol particles during the Azores Marine Aerosol and Gas Exchange, *J. Geophys. Res., 100,* 23,075-23,081, 1995.

Singh, H. B., and J. F. Kasting, Chlorine-hydrocarbon photochemistry in the marine troposphere and lower stratosphere, *J. Atmos. Chem., 7,* 261-285, 1988.

Singh, H. B., et al., Low ozone in the marine boundary layer of the tropical Pacific Ocean: Photochemical loss, chlorine atoms, and entrainment in Pacific Exploratory Mission-West, Phase A, *J. Geophys. Res., 101,* 1907-1917, 1996a.

Singh, H. B., A. N. Thakur, Y. E. Chen, and M. Kanakidou, Tetrachlorethene as an indicator of low Cl atom concentrations in the troposphere, *Geophys. Res. Lett., 23,* 1529-1532, 1996b.

Sorensen, S., H. Falbe-Hansen, M. Mangoni, J. Hjorth, and N. R. Jensen, Observation of DMSO and $CH_3S(O)OH$ from the gas phase reaction between DMS and OH, *J. Atmos. Chem., 24,* 299-315, 1996.

Stickel, R. E., J. M. Nicovich, S. Wang, Z. Zhao, and P. H. Wine, Kinetic and mechanistic study of the reaction of atomic chlorine with dimethyl sulfide, *J. Phys. Chem., 96,* 9875-9883, 1992.

Tang, I. N., Deliquescence properties and particle size change of hygroscopic aerosols, in *Generation of Aerosols*, edited by K. Willeke, chap. 7, pp. 153-167, Butterworth-Heinemann, Newton, Mass., 1980.

Tanner, D. J., and F. L. Eisele, Present OH measurement limits and associated uncertainties, *J. Geophys. Res., 100,* 2883, 1995.

Thompson, A. M., et al., Ozone observations and a model of marine boundary layer photochemistry during SAGA 3, *J. Geophys. Res., 98,* 16,955-16,968, 1993.

Turnipseed, A. A., S. B. Barone, and A. R. Ravishankara, Observation of CH_3S addition to O_2 in the gas phase, *J. Phys. Chem., 96,* 7502-7505, 1992.

Turnipseed, A. A., and A. R. Ravishankara, The Atmospheric Oxidation of Dimethyl Sulfide: Elementary Steps in a Complex Mechanism. In Restelli, G. and Angeletti, G., Eds., Dimethylsulphide: Oceans, Atmosphere and Climate, Kluwer, Dordrecht, 185-196, 1993.

Turnipseed, A. A., S. B. Barone, and A. R. Ravishankara, Reactions of OH with DMS, II, Products and mechanisms, *J. Phys. Chem., 100,* 14,703, 1996.

Tyndall, G. S., and A. R. Ravishankara, Kinetics of the reaction of CH_3S with O_3 at 298 K, *J. Phys. Chem., 93,* 4707-4710, 1989.

Veltwisch, D., E. Janata, and K. D. Asmus, Primary processes in the reaction of OH radicals with sulphoxides, *J. Chem. Soc. Perkin Trans. 2,* 146-153, 1980.

Wallington, T. J., E. Thomas, and O. J. Nielsen, Atmospheric chemistry of dimethyl sulfide: UV spectra and self-reaction kinetics of $CH_3SCH_2O_2$ radicals and kinetics of the reactions $CH_3SC\,H_2 + NO \rightarrow CH_3SCH_2O + NO_2$, and $CH_3SCH_2O_2 + NO \rightarrow CH_3SCH_2O + NO_2$, *J. Phys. Chem., 97,* 8442-8449, 1993.

Warneck, P., *Chemistry of the Natural Atmosphere*, Academic, San Diego, Calif., 1988.

Wingenter, O. W., M. K. Kubo, N. J. Blake, T. W. Smith, D. R. Blake, and F. S. Rowland, Hydrocarbon and halocarbon measurements as photochemical and dynamical indicators of atmospheric hydroxyl, atomic chlorine, and vertical mixing obtained during Lagrangian flights, *J. Geophys. Res., 101,* 4331-4340, 1996.

Yvon, S. A., E. S. Saltzman, D. J. Cooper, T. S. Bates, and A. M. Thompson, Atmospheric sulfur cycling in the tropical Pacific marine boundary layer (12°S, 135°W): A comparison of field data and model results, I, Dimethylsulfide, *J. Geophys. Res., 101,* 6899-6909, 1996a.

Yvon, S. A., E. S. Saltzman, D. J. Cooper, T. S. Bates, and A. M. Thompson, Atmospheric sulfur cycling in the tropical Pacific marine boundary layer (12°S, 135°W): A comparison of field data and model results, 2, Sulfur dioxide, *J. Geophys. Res., 101,* 6911-6918, 1996b.

Zhao, Z., R. E. Stickel, and P. H. Wine, Branching ratios for methyl elimination in the reactions of $O(^1D)$ radicals and Cl atoms with CH_3SCH_3, *Chem. Phys. Lett., 251,* 59-66, 1996.

A. Bandy and D. Thornton, Department of Chemistry, Drexel University, Philadelphia, PA 19104.

D. Blake, Department of Chemistry, University of California, Irvine, CA 92697.

G. Chen and D. Davis, School of Earth and Atmospheric Sciences, Georgia Institute of Technology, Atlanta, GA 30332. (e-mail: douglas.davis@eas.gatech.edu).

A. Clarke, J. Heath, and B. Huebert, Department of Oceanography, University of Hawaii, Honolulu, HI 96822.

F. Eisele, D. Lenschow, L. Mauldin, and D. Tanner, National Center for Atmospheric Research, Boulder, CO 80307.

H. Fuelbert, Meteorolgy Department, Florida State University, Tallahassee, FL 32306.

(Received October 31, 1997; revised July 10, 1998; accepted August 17, 1998.)